Figure 4.73 NORTH529 – East & Vertical Components – Base Residual Horizontal Displacement

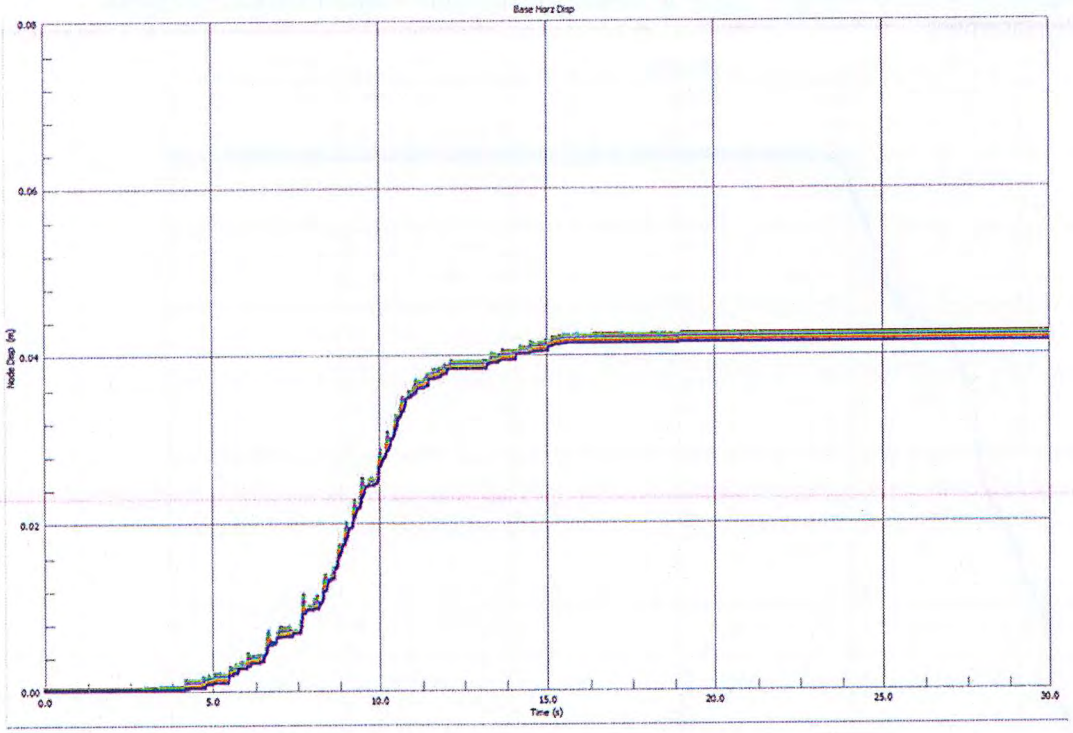

Figure 4.74 NORTH529 – North & Vertical Components – Base Residual Horizontal Displacement

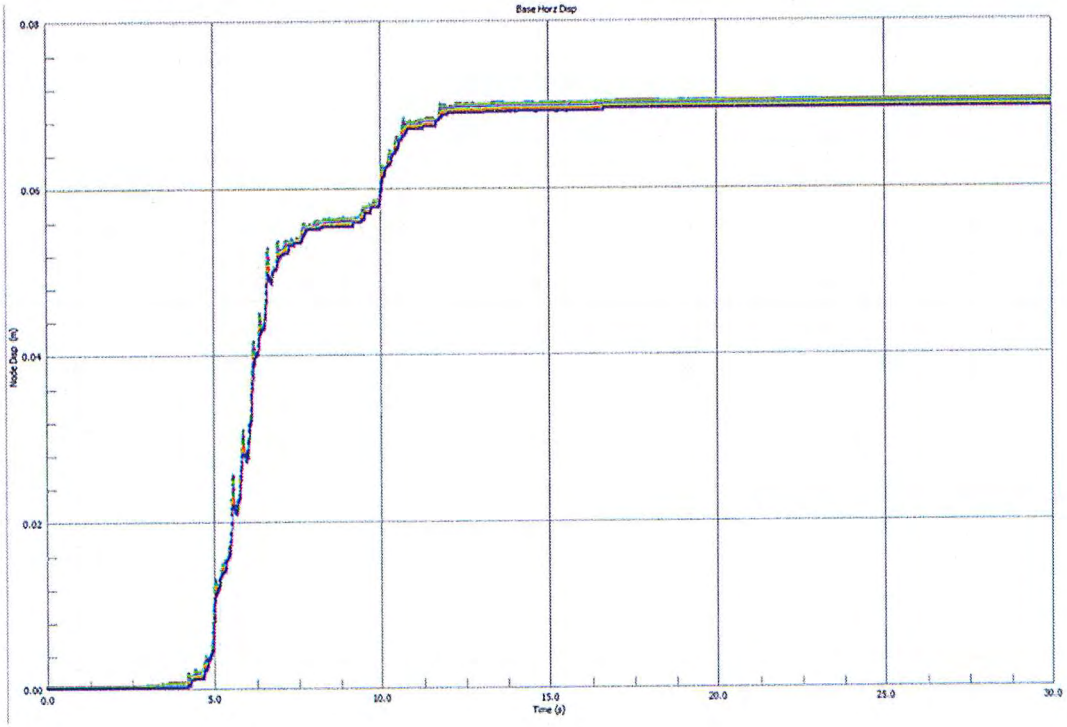

Figure 4.75 NORTH-WON – South & Vertical Components – Base Residual Horizontal Displacement

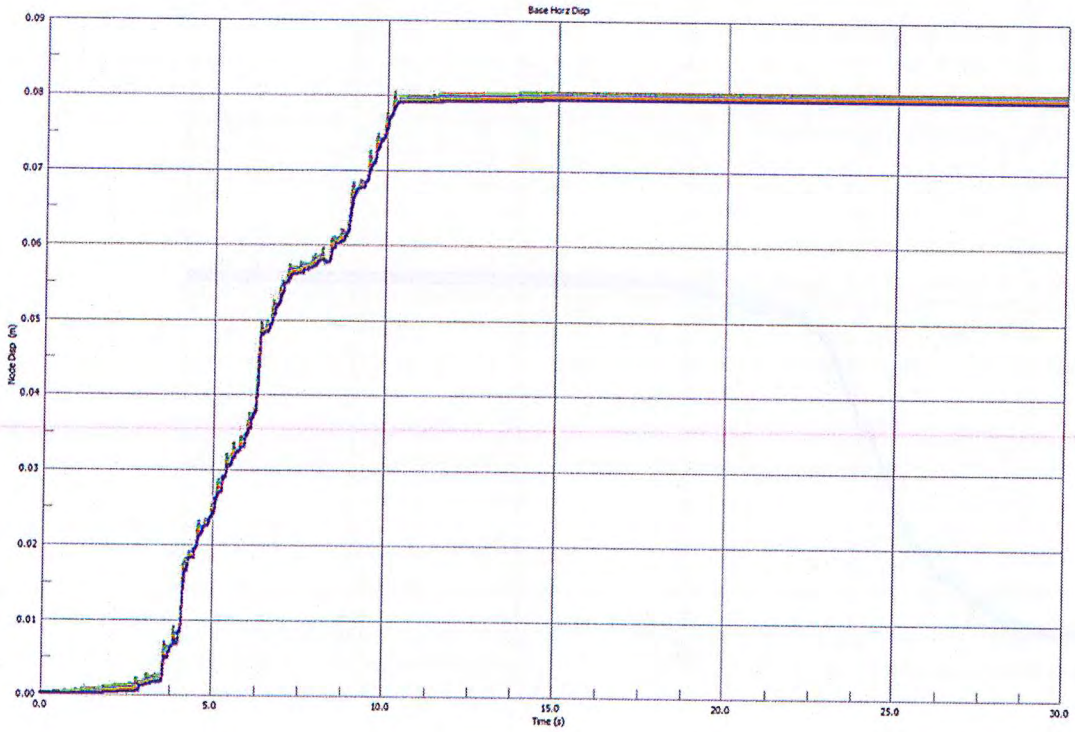

Figure 4.76 NORTH-WON – West & Vertical Components – Base Residual Horizontal Displacement

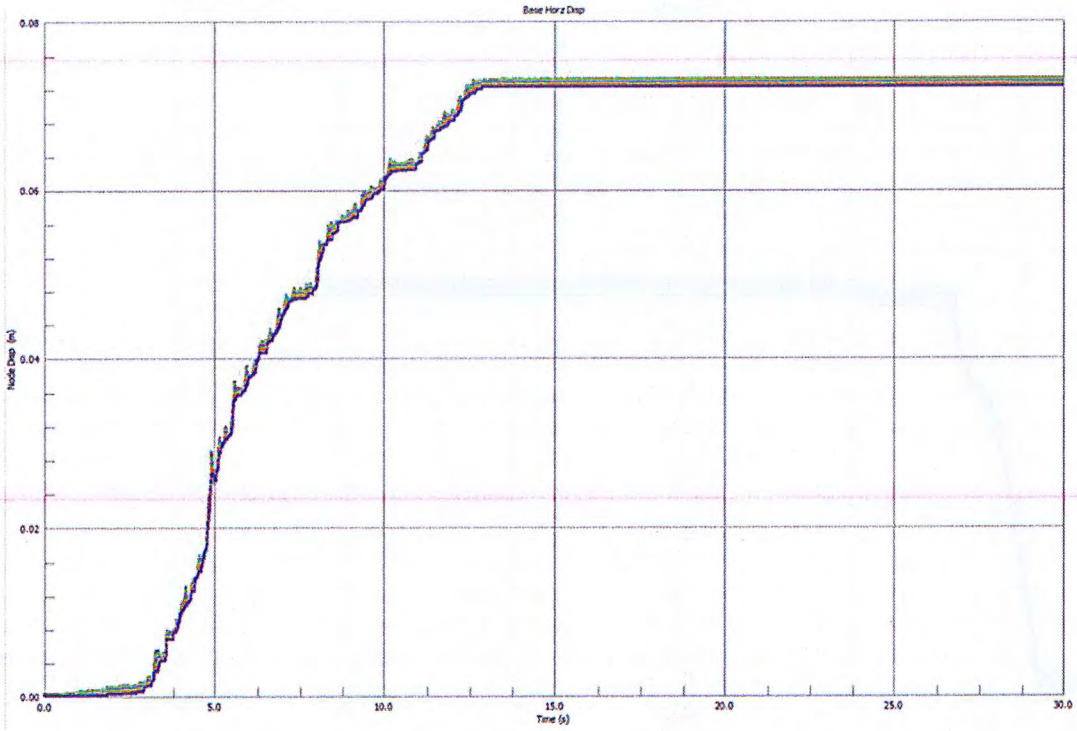

Figure 4.77 SMADRE-4734 – North & Vertical Components – Base Residual Horizontal Displacement

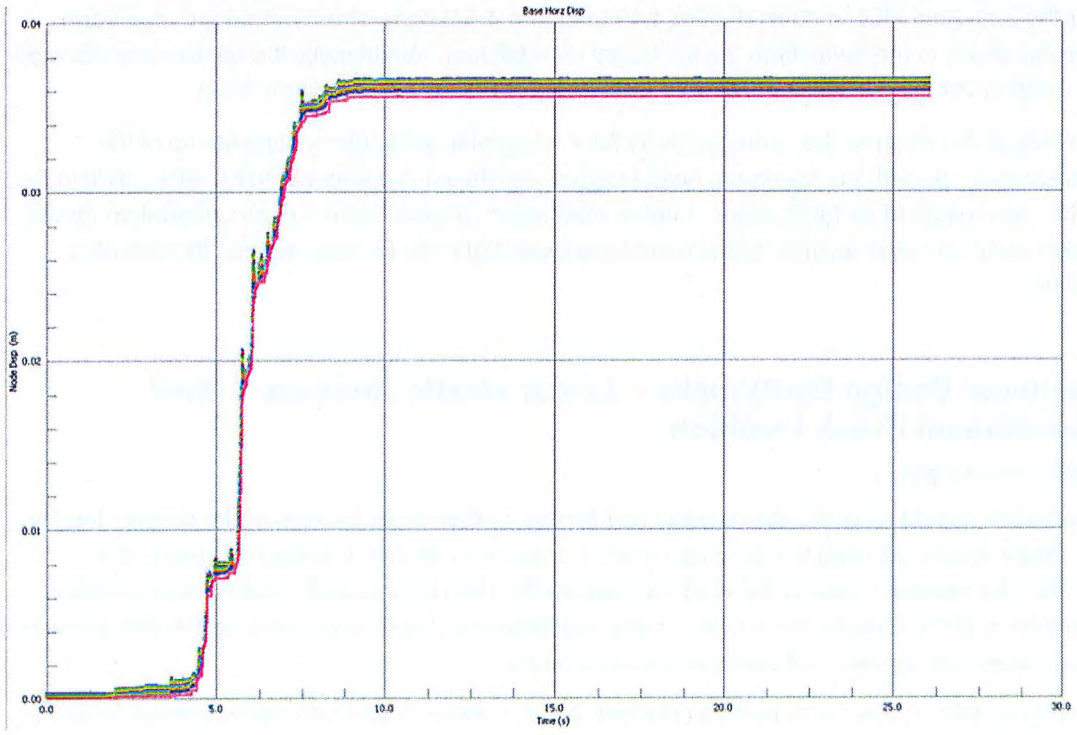

Figure 4.78 SMADRE-4734 – West & Vertical Components – Base Residual Horizontal Displacement

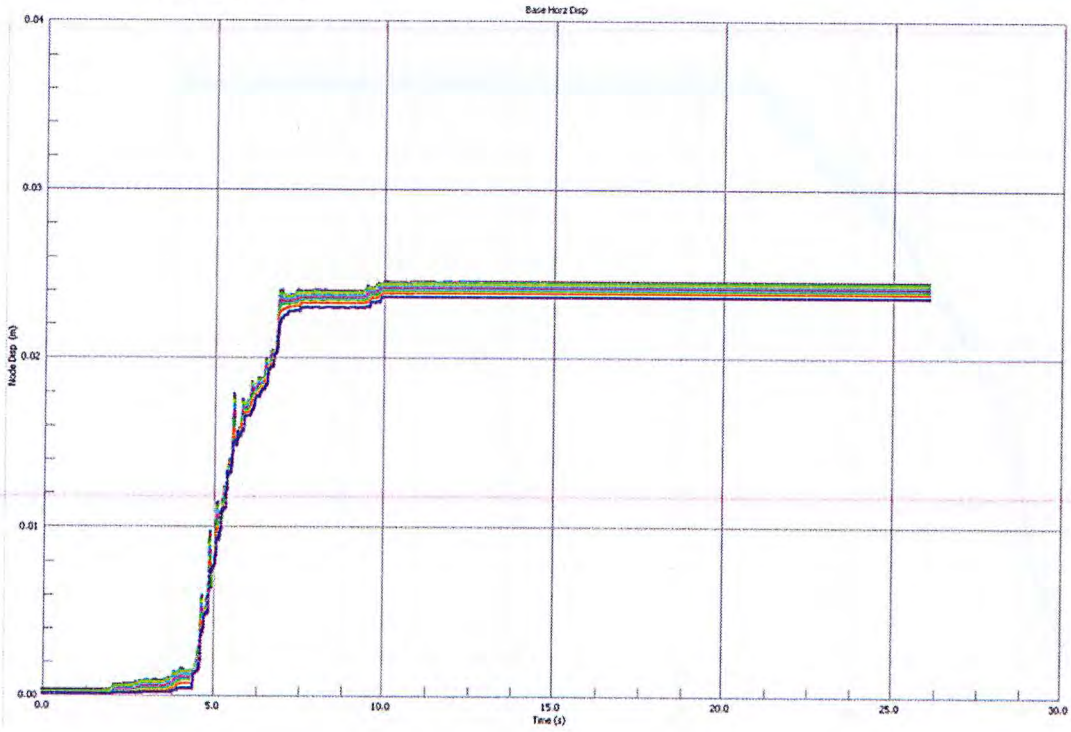

4.4.3 Discussion – Abutment Sections

The results for the abutment MDE models (Figure 4.49 to Figure 4.72) show stresses that are of a lesser magnitude in comparison to the result from the full height dam section. Additionally the relative displacement at the dam foundation interface is also appreciably smaller (refer Figure 4.73 to Figure 4.78).

The stress envelopes do not show the same proclivity for a horizontal crack intercepting the tip of the assumed vertical crack. As with the maximum height section significant cracking would be anticipated in the abutment section as a result of an MDE event. Further non-linear analysis has not been undertaken for the abutment model, given any post seismic displacement are expected to be less server than those for the maximum section.

4.5 Maximum Design Earthquake – Linear elastic Analysis – Most Downstream Crack Location

4.5.1 Stress Envelopes

In order to assess the sensitivity of the dam's behaviour for the vertical crack location under seismic loading, the maximum height model including the assumed vertical crack from RL 510.8 to the foundation at a location 23 m from the upstream face of the dam (as opposed to 15 m for the other models) was analysed. Only the North-Won and the SMadre-4734 events were considered as these generated the highset stresses in the analyses undertaken for the most upstream crack location.

Figure 4.79 to Figure 4.84 shows the maximum principal stress, maximum principal stress direction and the maximum vertical stress envelopes for the MDE load cases undertaken with the maximum height model

Figure 4.85 to Figure 4.86 provides graphs of the relative displacement of the non-linear elements along the dam foundation interface for each of the MDE events.

North-Won Maximum Design Earthquake

Figure 4.79 NORTH-WON – West & Vertical Components – Maximum Stress Envelope – Maximum Principal Stress

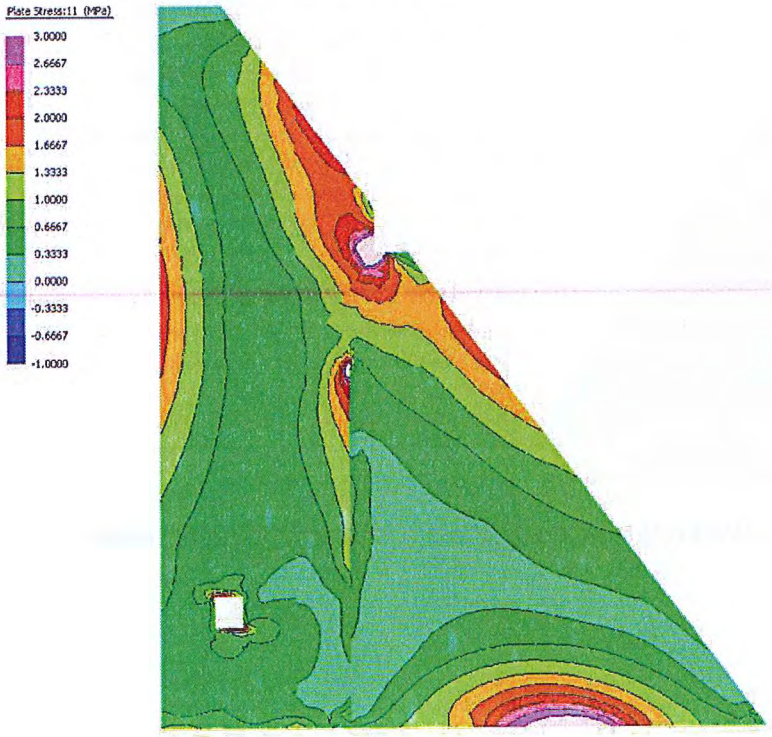

Figure 4.80 NORTH-WON – West & Vertical Components – Maximum Stress Envelope – Maximum Principal Stress Direction

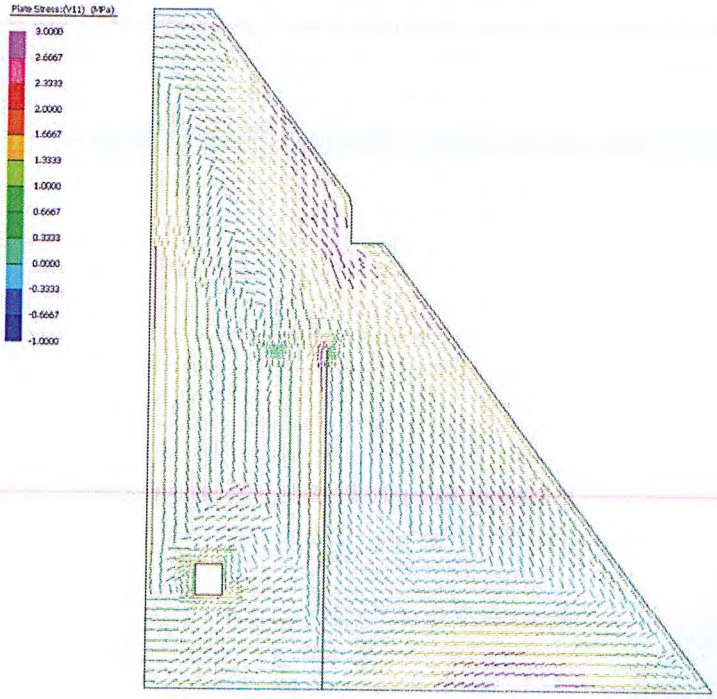

Figure 4.81 NORTH-WON – West & Vertical Components – Maximum Stress Envelope – Vertical Stress

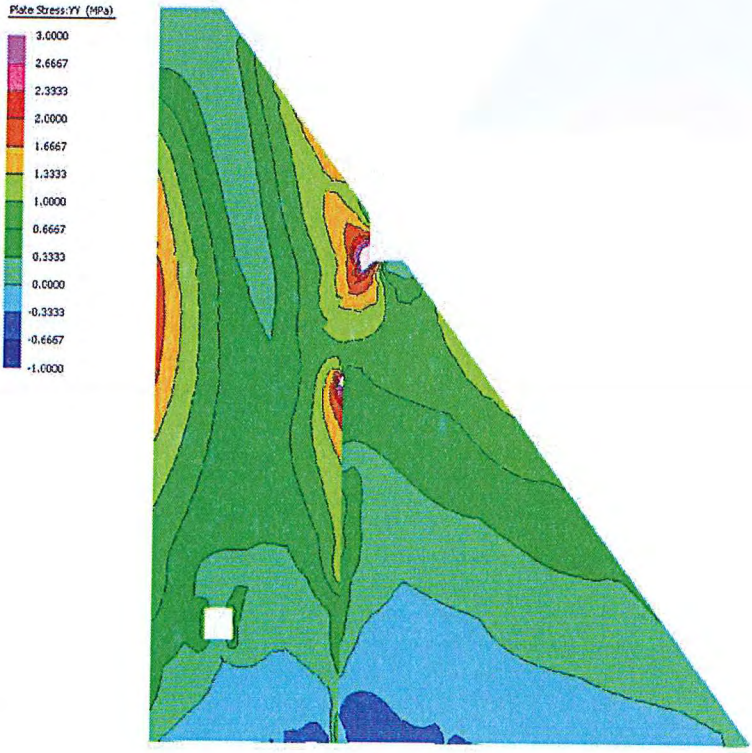

SMadre-4734 Maximum Design Earthquake

Figure 4.82 SMADRE-4734 – North & Vertical Components – Maximum Stress Envelope – Maximum Principal Stress

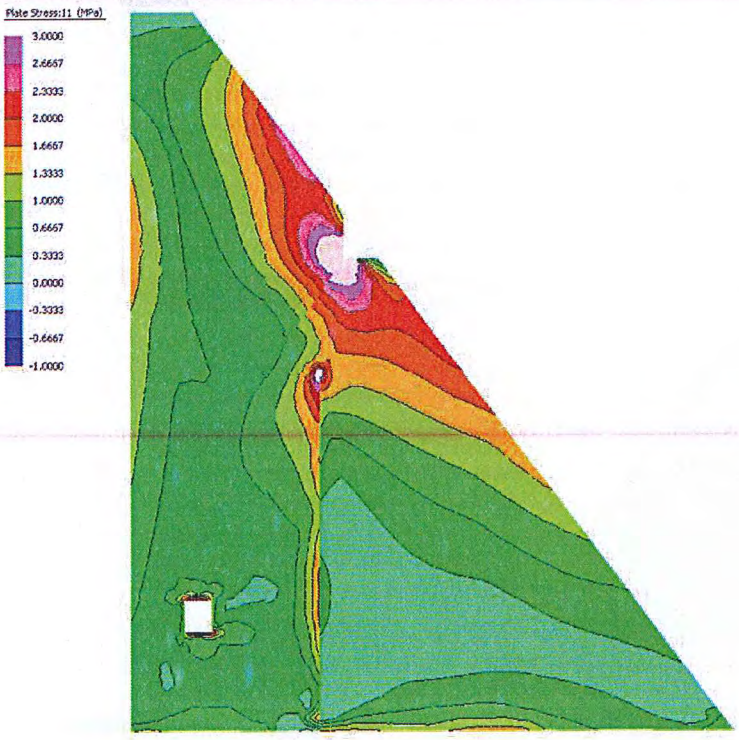

Figure 4.83 SMADRE-4734 – North & Vertical Components – Maximum Stress Envelope – Maximum Principal Stress Direction

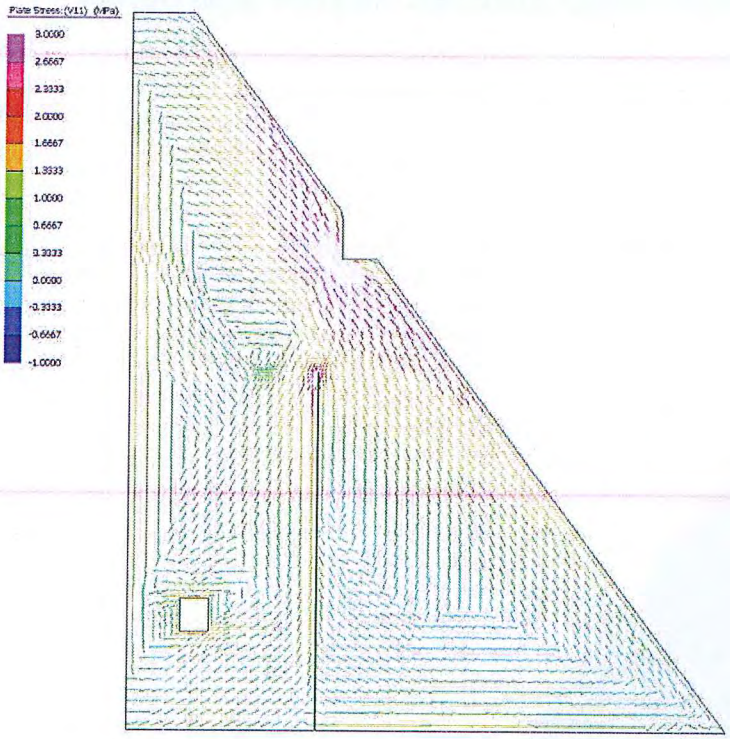

Figure 4.84 SMADRE-4734 – North & Vertical Components – Maximum Stress Envelope – Vertical Stress

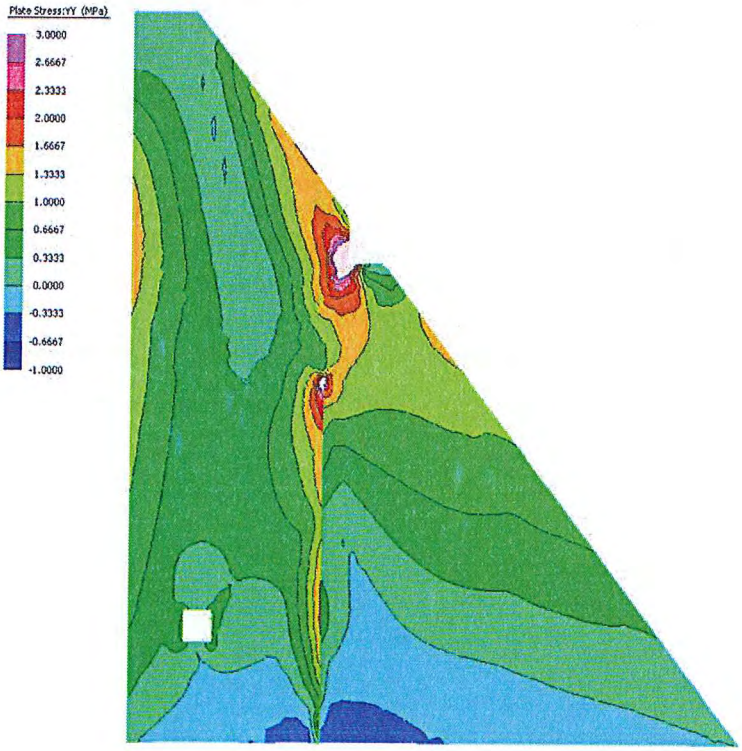

4.5.2 Displacement charts

North-Won Maximum Design Earthquake

Figure 4.85 NORTH-WON – West & Vertical Components – Base Residual Horizontal Displacement

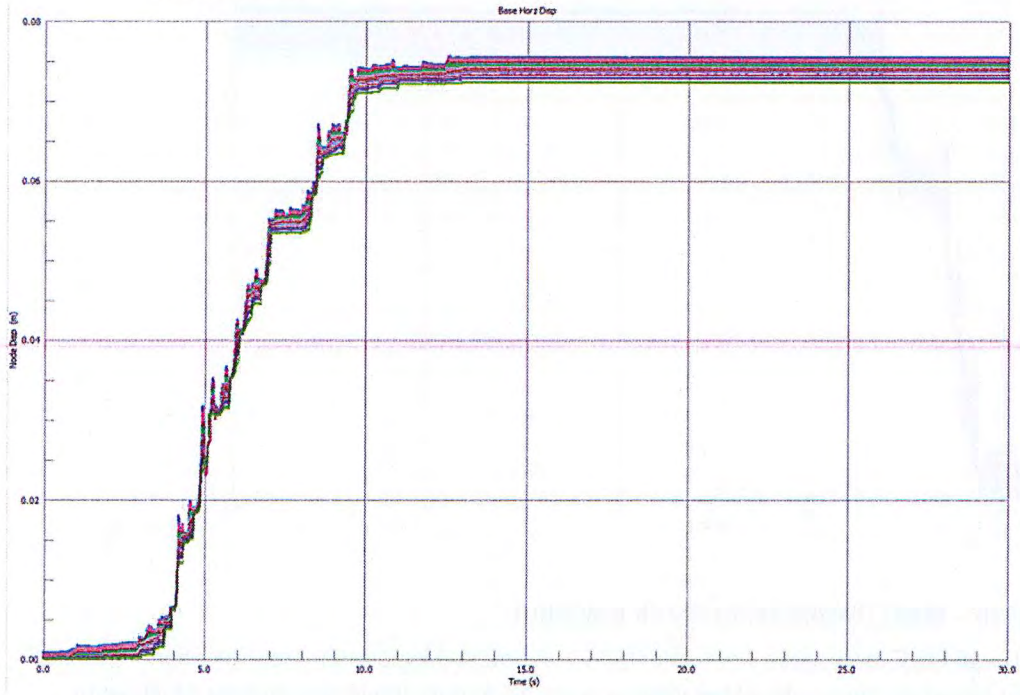

Figure 4.86 SMADRE-4734 – North & Vertical Components – Base Residual Horizontal Displacement

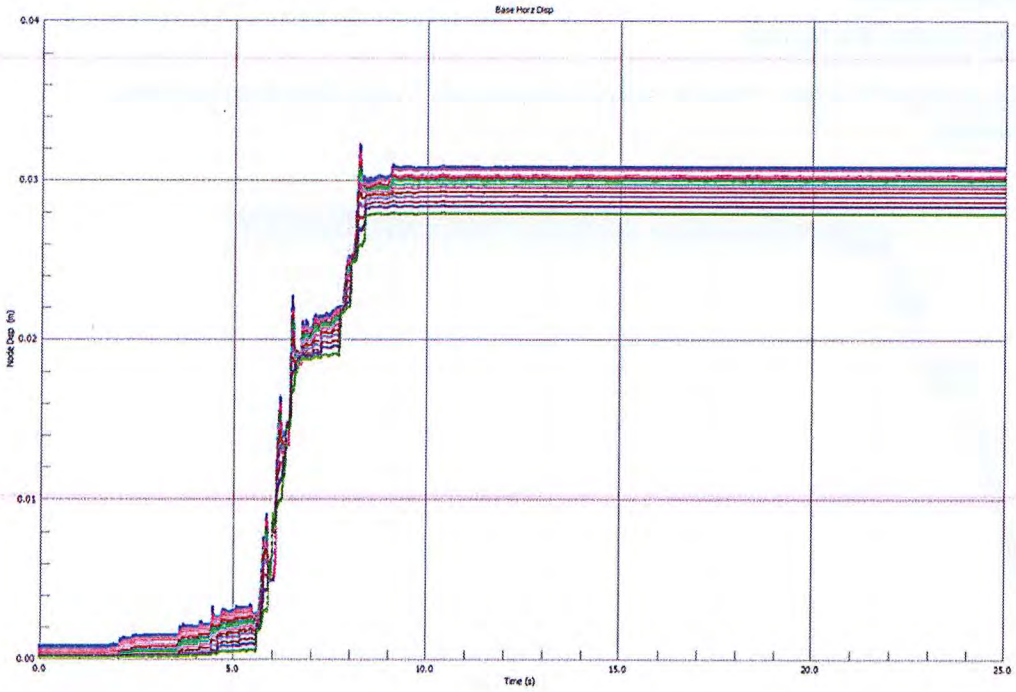

4.5.3 Discussion – Most Downstream Crack Location

Only a limited number of MDE load cases were selected for the most downstream crack location. The MDE cases were selected based on the results of the vertical crack 15 m from the upstream face which were observed to have the highest tensile stresses and largest displacements at the dam foundation interface. In general the results for the downstream crack location (Figure 4.79 to Figure 4.86) show an increased area of high stress between the tip of the crack and the upstream in addition to an increase in the residual displacement at the dam foundation interface. These changes were not considered to be significant enough for further non-linear analysis in addition to what has been carried out for the assumed crack located 15m from the upstream face.

4.6 Maximum Design Earthquake – Non- Linear Analysis

4.6.1 Stress Envelopes

Figure 4.87 to Figure 4.110 show:

- the maximum principal stress and the maximum vertical stress envelopes for the MDE load cases undertaken for the non-linear analysis. (Note – plots of maximum principal stress envelopes are a summary plot of the maximum principal stress recorded at each node. As such the maximum stress at any node may occur at any time step during the analysis period, and does may not necessarily occur at the same time step for all nodes) and;
- maximum principal stress and maximum principal stress direction for the time step where the horizontal crack is at its maximum open position (nominally the maximum d/s deflection of the crest)

This analysis assumes that a full depth horizontal crack has developed at RL 551.3 m AHD (510.8 m AHD in the model) and intersects the top of the vertical crack

Figure 4.111 to Figure 4.140 provides graphs for each of the MDE events of the relative displacement of the non-linear elements along the dam foundation interface, the vertical crack from RL 510.8 to the foundation, and the crack horizontal crack from upstream to downstream at RL 510.8.

Figure 4.87 NORTH529 – East & Vertical Components – Maximum Stress Envelope – Maximum Principal Stress

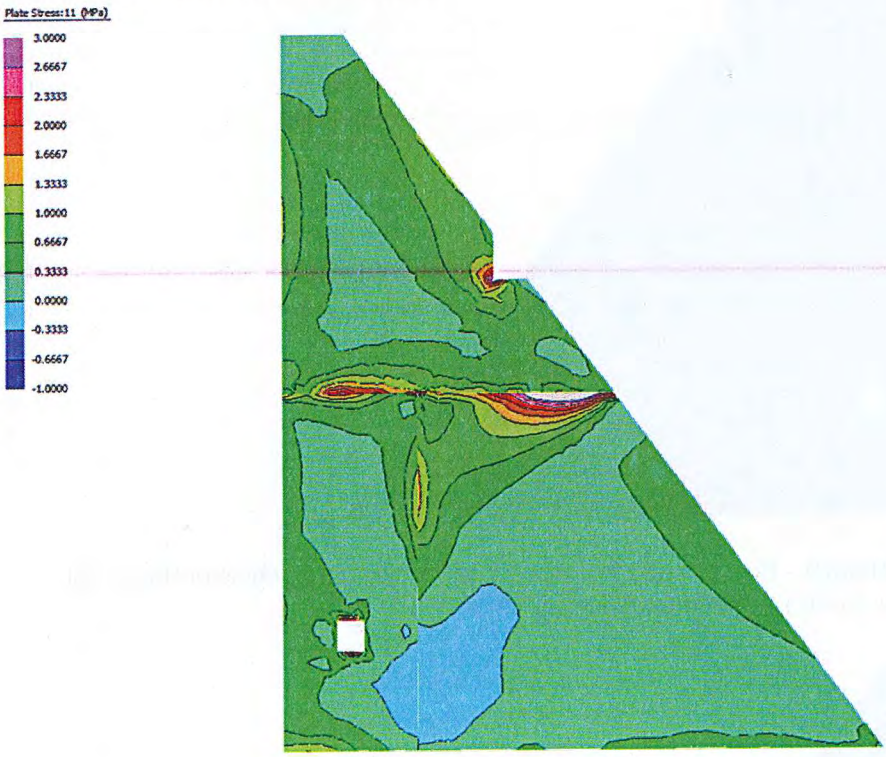

Figure 4.88 NORTH529 – East & Vertical Components – Maximum Stress Envelope – Vertical Stress

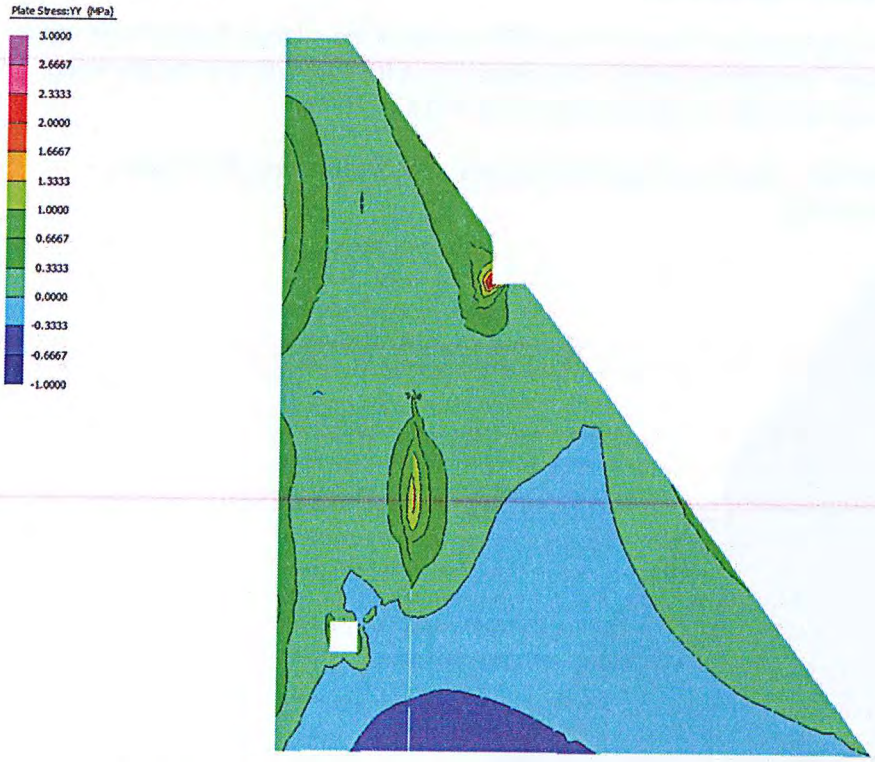

Figure 4.89 NORTH529 – East & Vertical Components – Maximum Opening of Horizontal Crack at U/S Face (5.11s) – Maximum Principal Stress

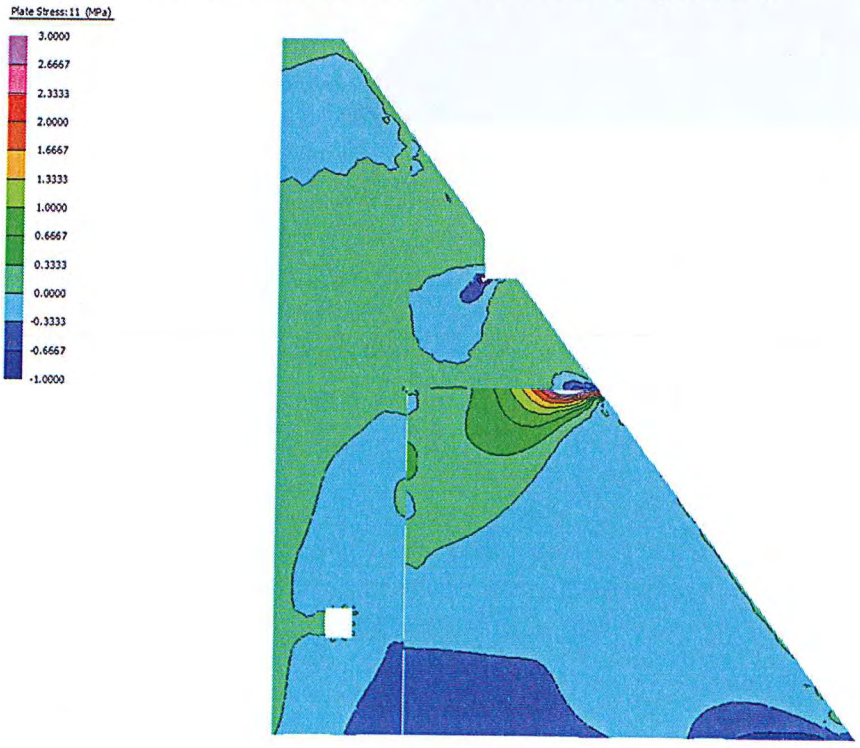

Figure 4.90 NORTH529 – East & Vertical Components – Maximum Opening of Horizontal Crack at U/S Face (5.11s) – Maximum Principal Stress Direction

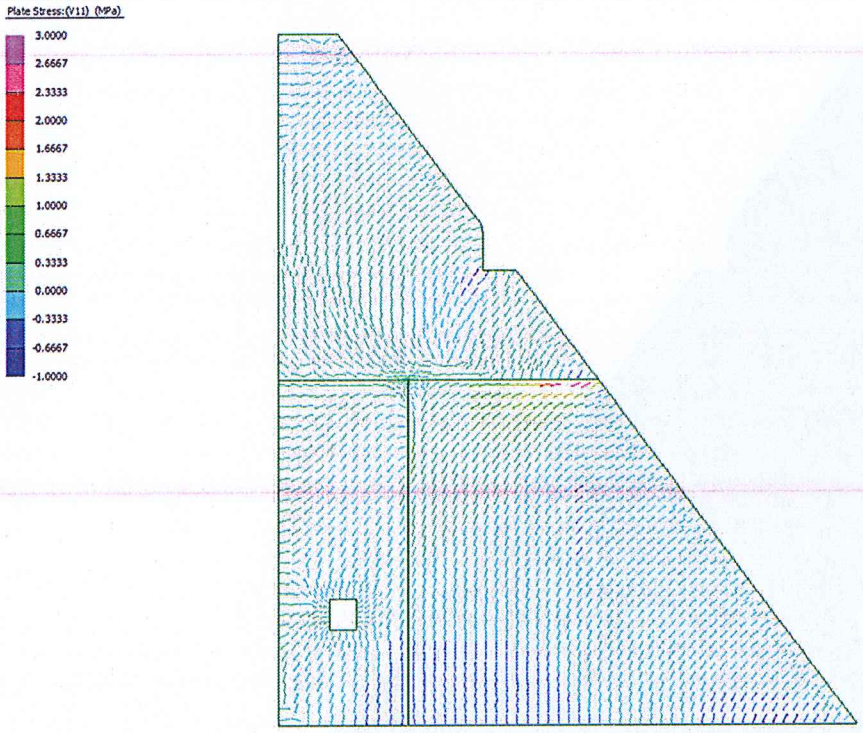

Figure 4.91 NORTH529 – North & Vertical Components – Maximum Stress Envelope – Maximum Principal Stress

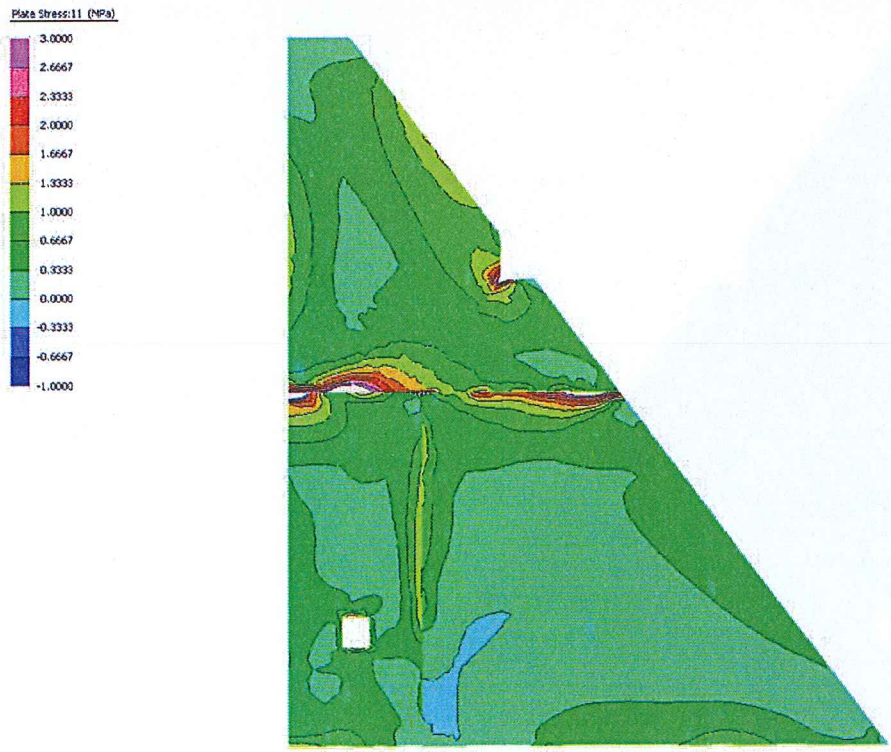

Figure 4.92 NORTH529 – North & Vertical Components – Maximum Stress Envelope – Vertical Stress

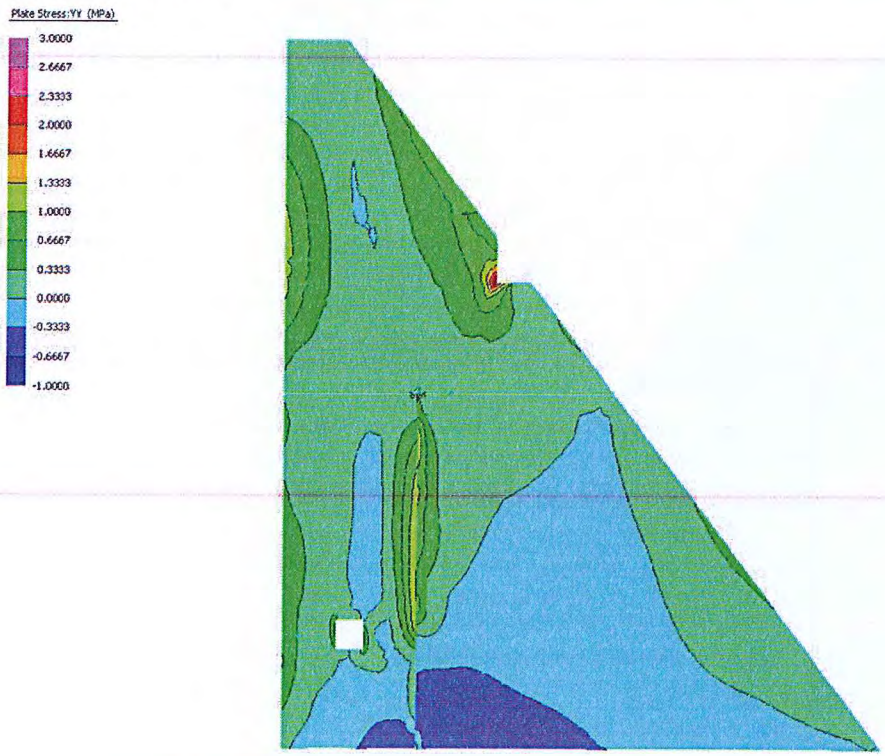

Figure 4.93 NORTH529 – North & Vertical Components – Maximum Opening of Horizontal Crack at U/S Face (6.79s) – Maximum Principal Stress

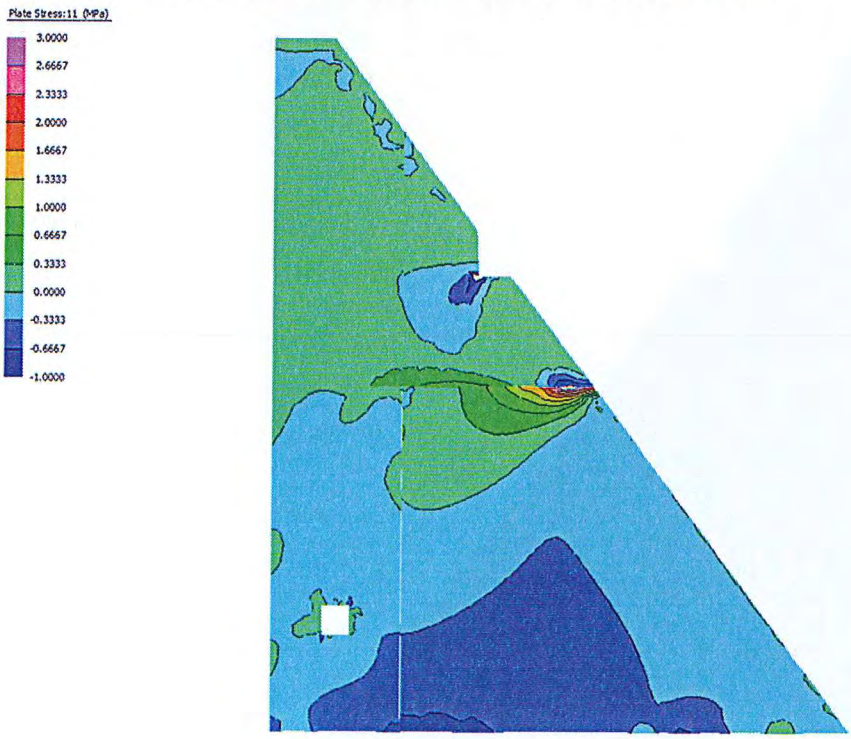

Figure 4.94 NORTH529 – North & Vertical Components – Maximum Opening of Horizontal Crack at U/S Face (6.79s) – Maximum Principal Stress Direction

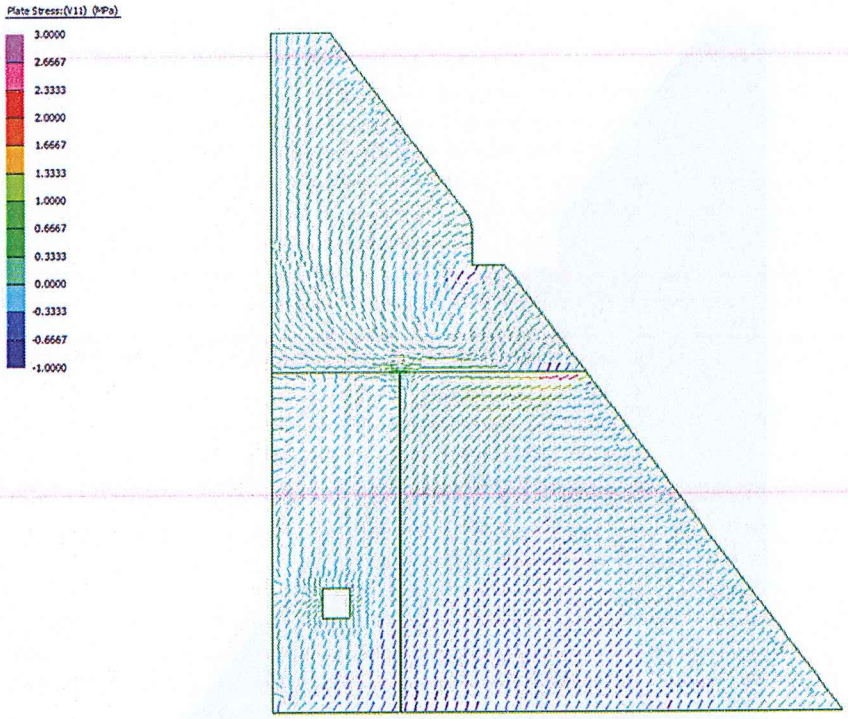

Figure 4.95 NORTH-WON – South & Vertical Components – Maximum Stress Envelope – Maximum Principal Stress

Figure 4.96 NORTH-WON – South & Vertical Components – Maximum Stress Envelope – Vertical Stress

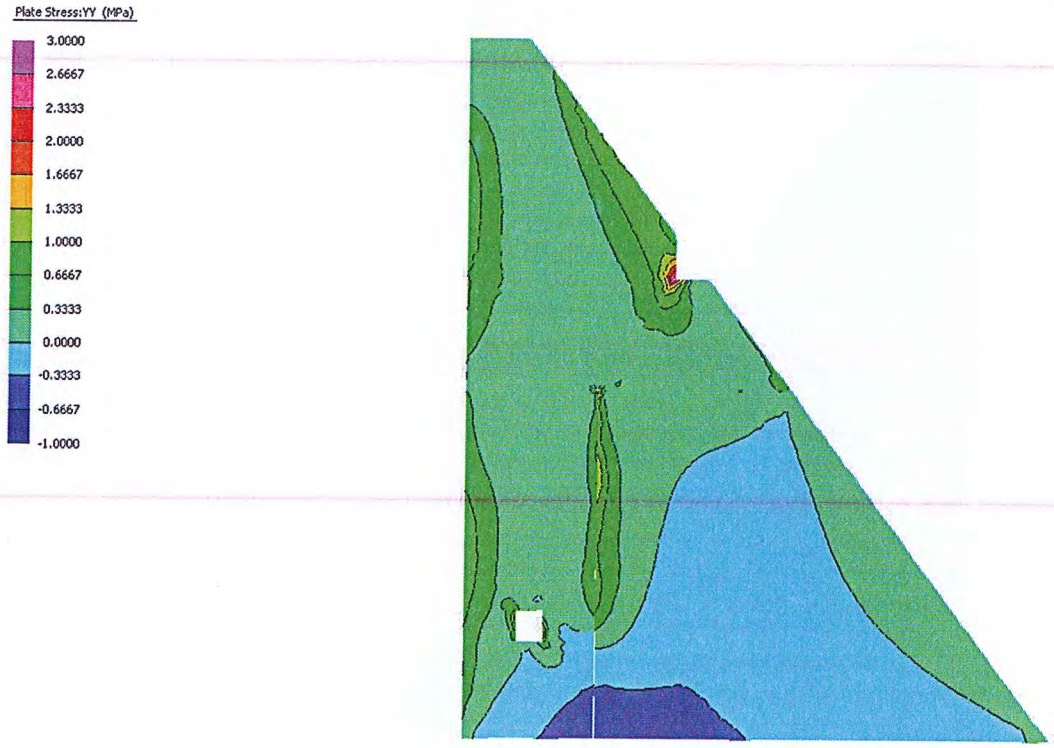

Figure 4.97 NORTH-WON – South & Vertical Components – Maximum Opening of Horizontal Crack at U/S Face (8.805s) – Maximum Principal Stress

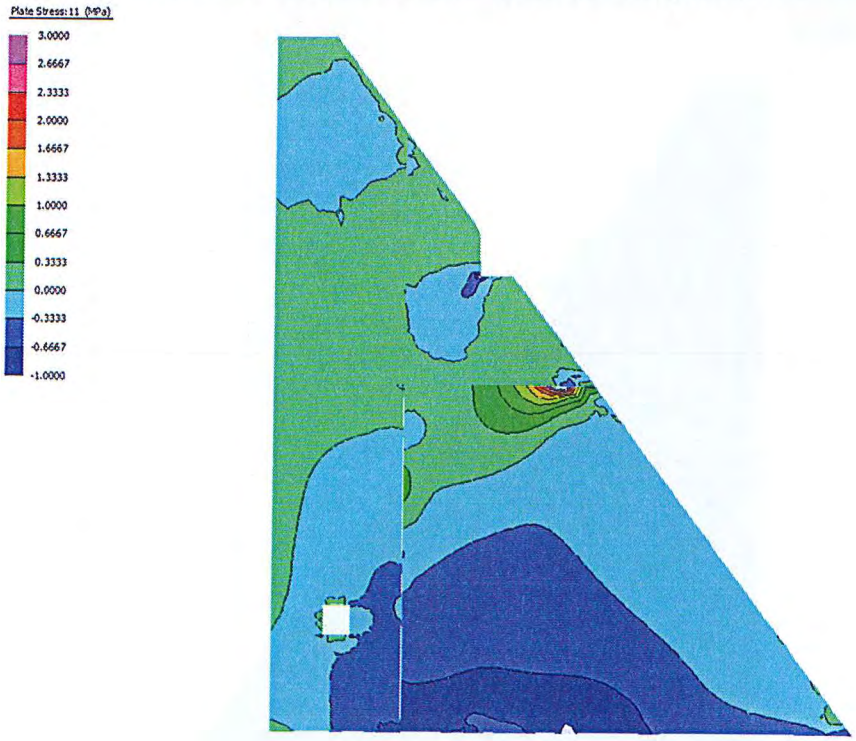

Figure 4.98 NORTH-WON – South & Vertical Components – Maximum Opening of Horizontal Crack at U/S Face (8.805s) – Maximum Principal Stress Direction

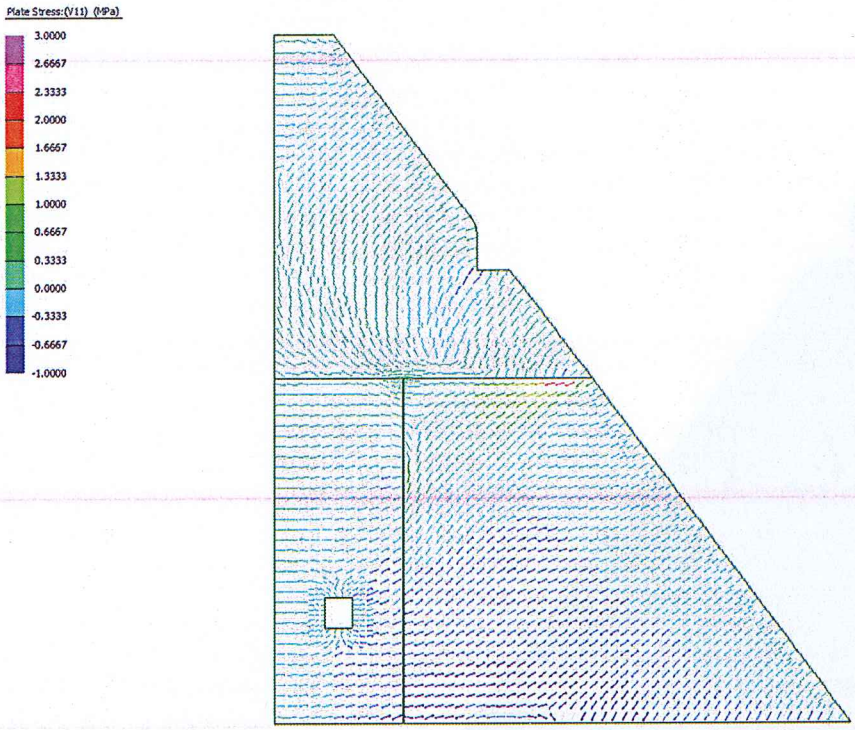

Figure 4.99 NORTH-WON – West & Vertical Components – Maximum Stress Envelope – Maximum Principal Stress

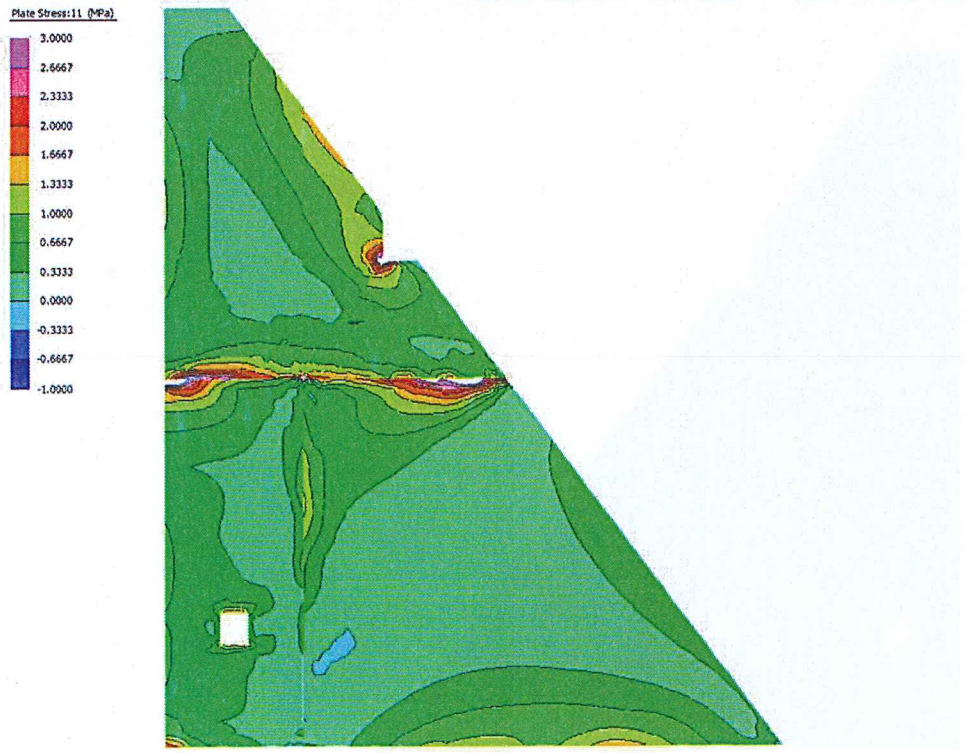

Figure 4.100 NORTH-WON – West & Vertical Components – Maximum Stress Envelope – Vertical Stress

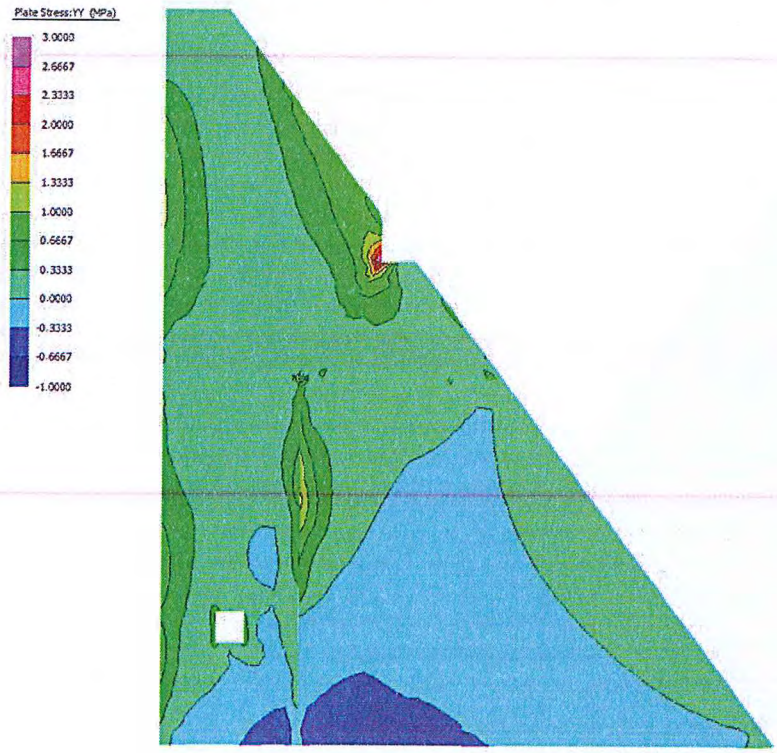

Figure 4.101 NORTH-WON – West & Vertical Components – Maximum Opening of Horizontal Crack at U/S Face (8.18s) – Maximum Principal Stress

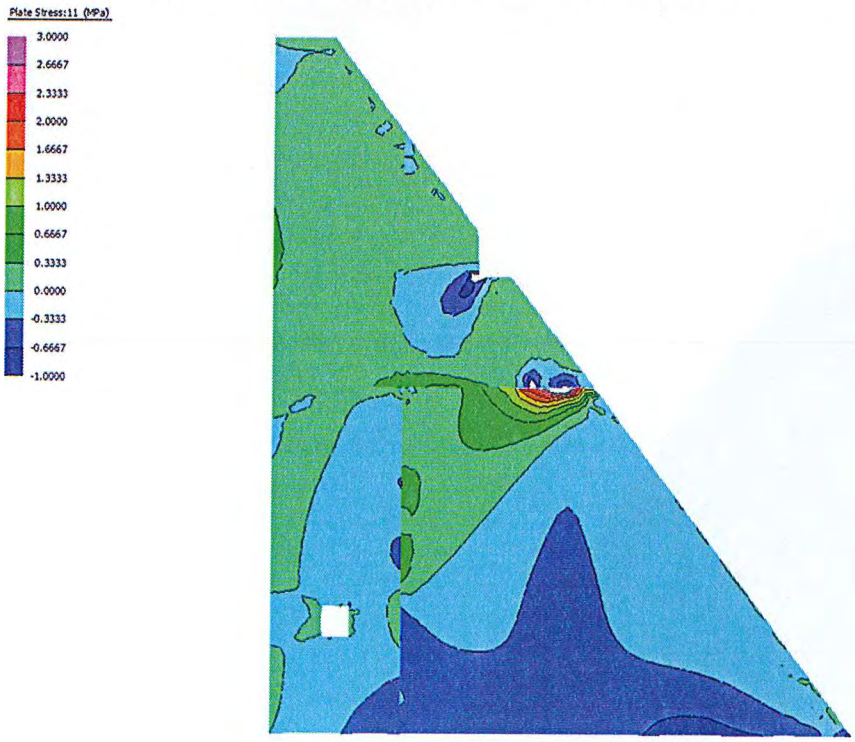

Figure 4.102 NORTH-WON – West & Vertical Components – Maximum Opening of Horizontal Crack at U/S Face (8.18s) – Maximum Principal Stress Direction

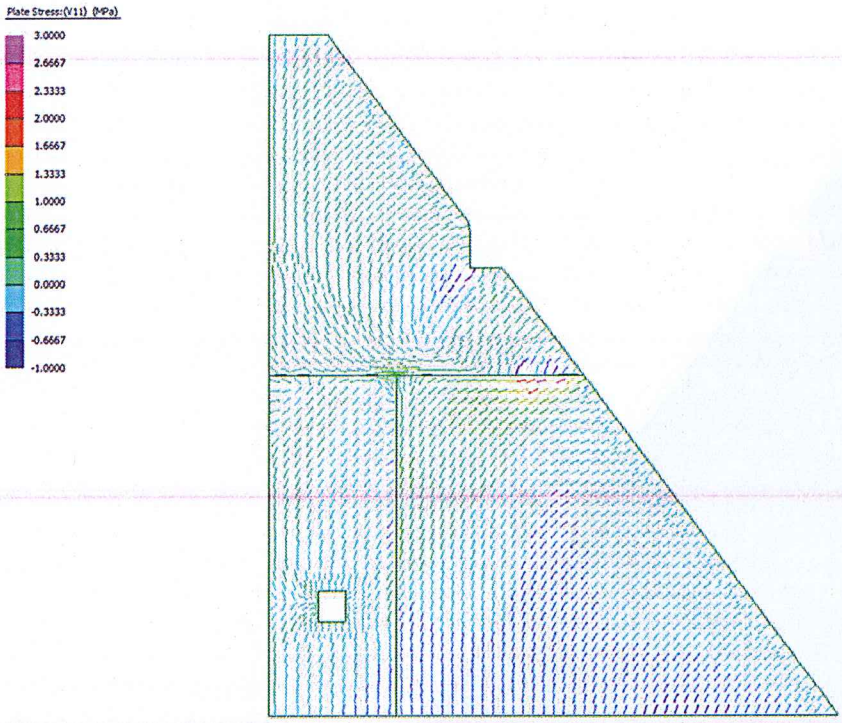

Figure 4.103 SMADRE-4734 – North & Vertical Components – Maximum Stress Envelope – Maximum Principal Stress

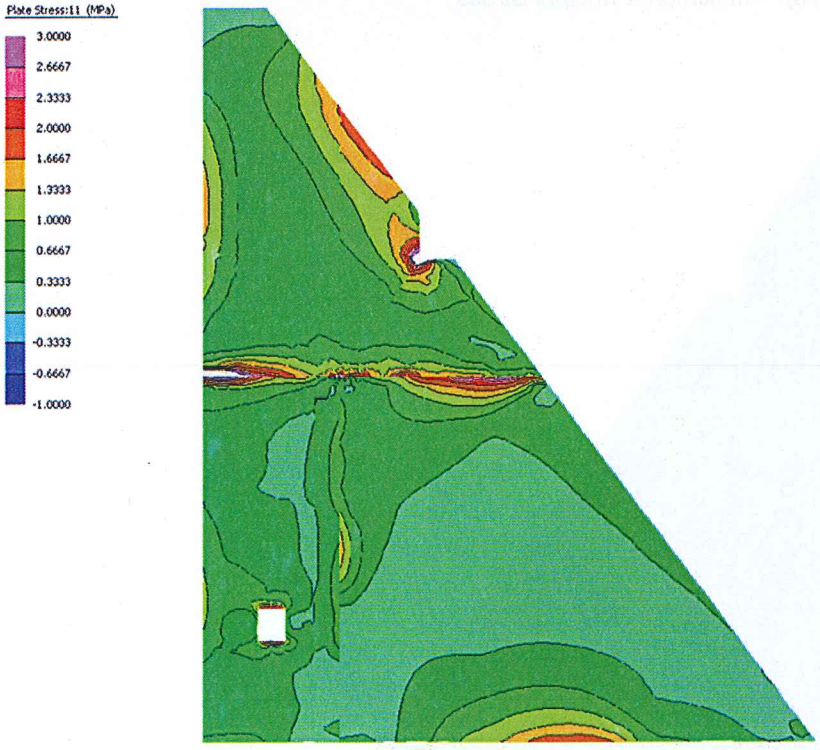

Figure 4.104 SMADRE-4734 – North & Vertical Components – Maximum Stress Envelope – Vertical Stress

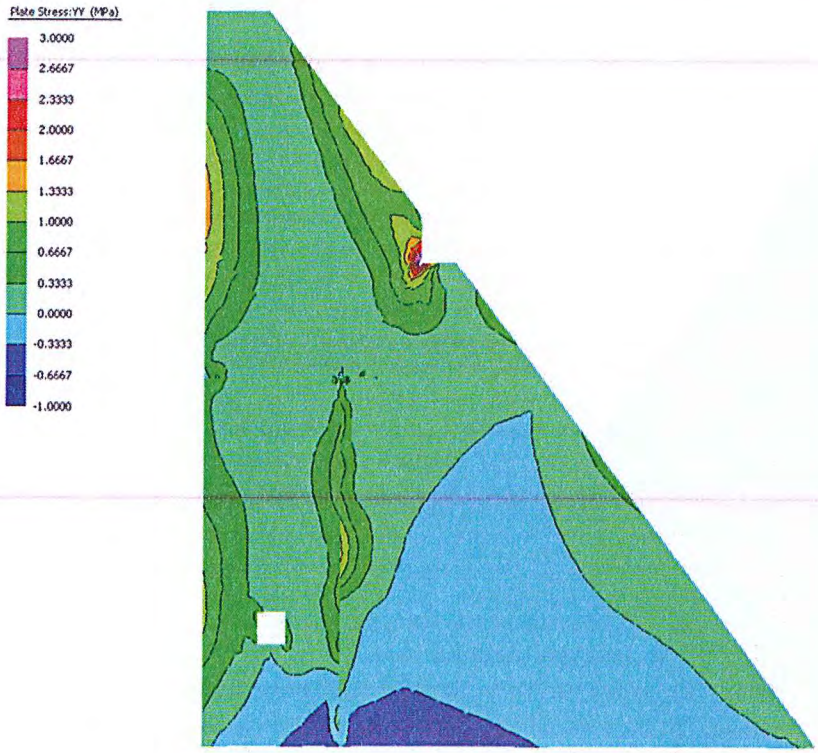

Figure 4.105 SMADRE-4734 – North & Vertical Components – Maximum Opening of Horizontal Crack at U/S Face (6.47s) – Maximum Principal Stress

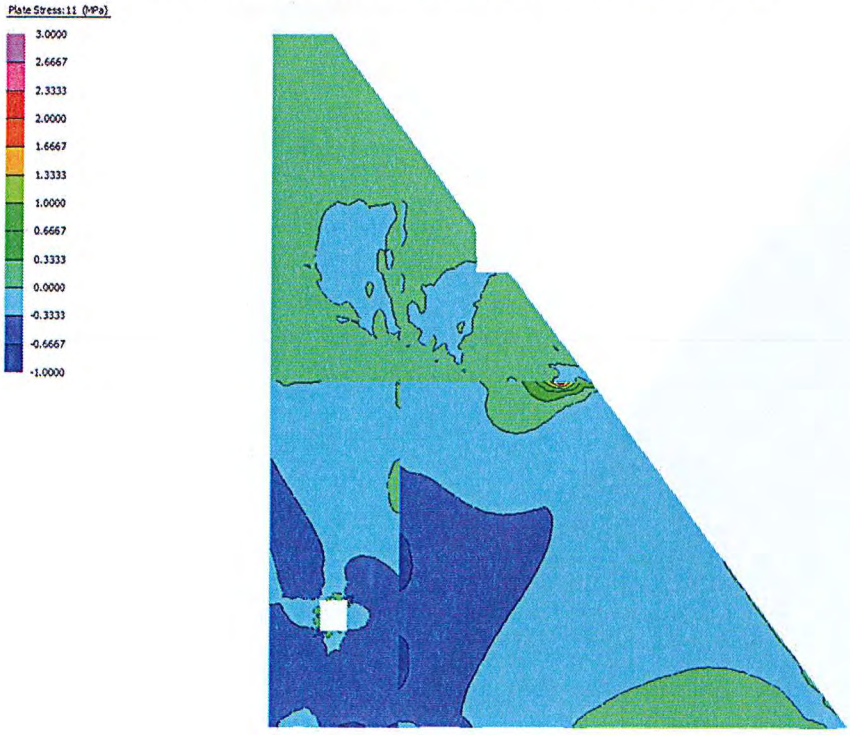

Figure 4.106 SMADRE-4734 – North & Vertical Components – Maximum Opening of Horizontal Crack at U/S Face (6.47s) – Maximum Principal Stress Direction

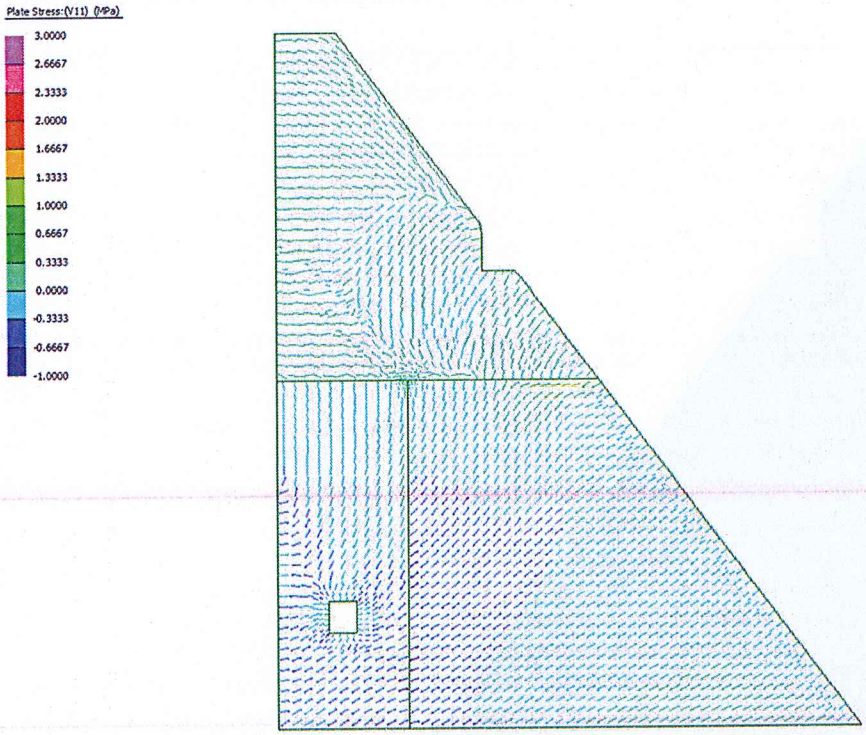

Figure 4.107 SMADRE-4734 – West & Vertical Components – Maximum Stress Envelope – Maximum Principal Stress

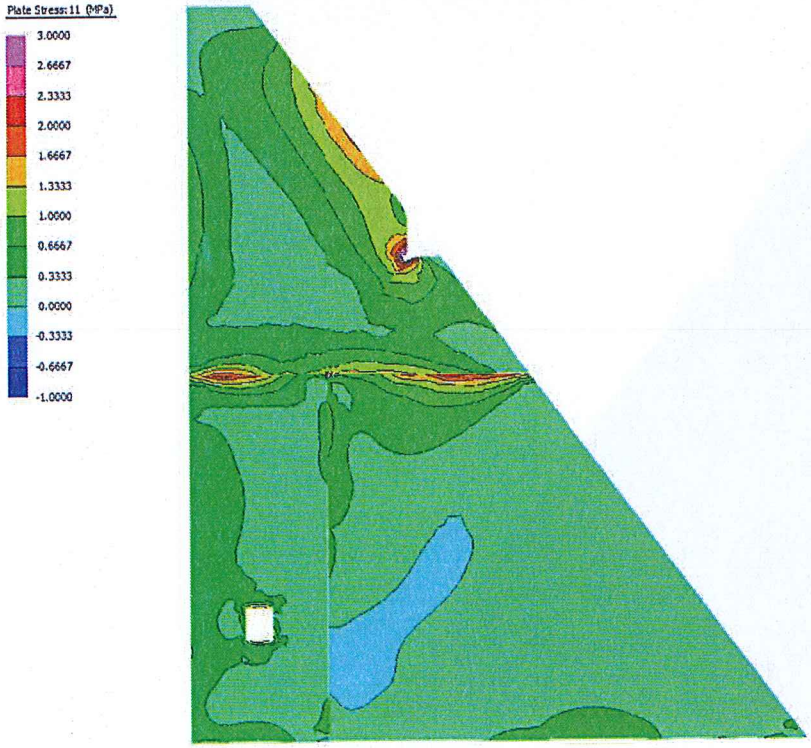

Figure 4.108 SMADRE-4734 – West & Vertical Components – Maximum Stress Envelope – Vertical Stress

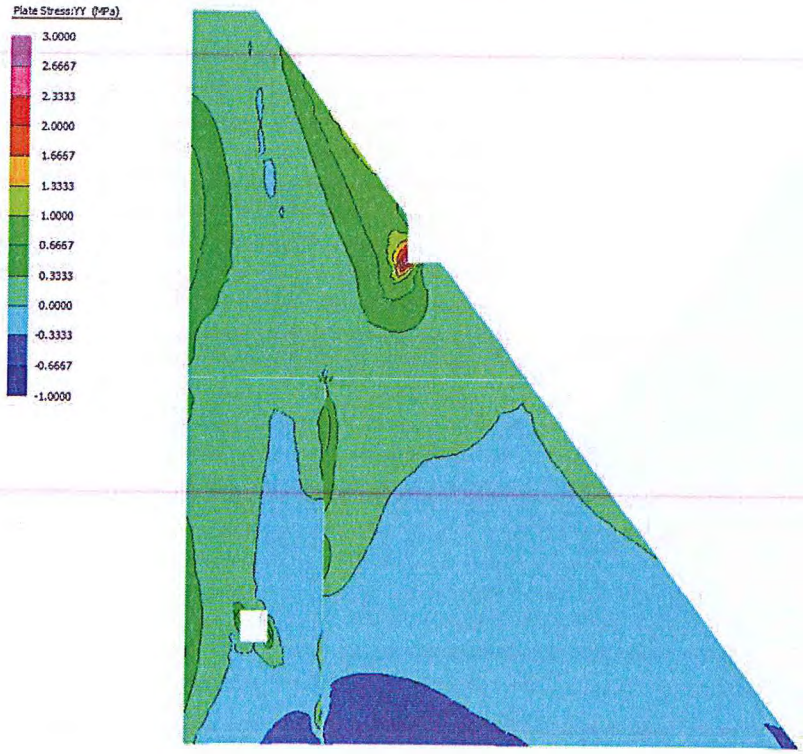

Figure 4.109 SMADRE-4734 – West & Vertical Components – Maximum Opening of Horizontal Crack at U/S Face (4.98s) – Maximum Principal Stress

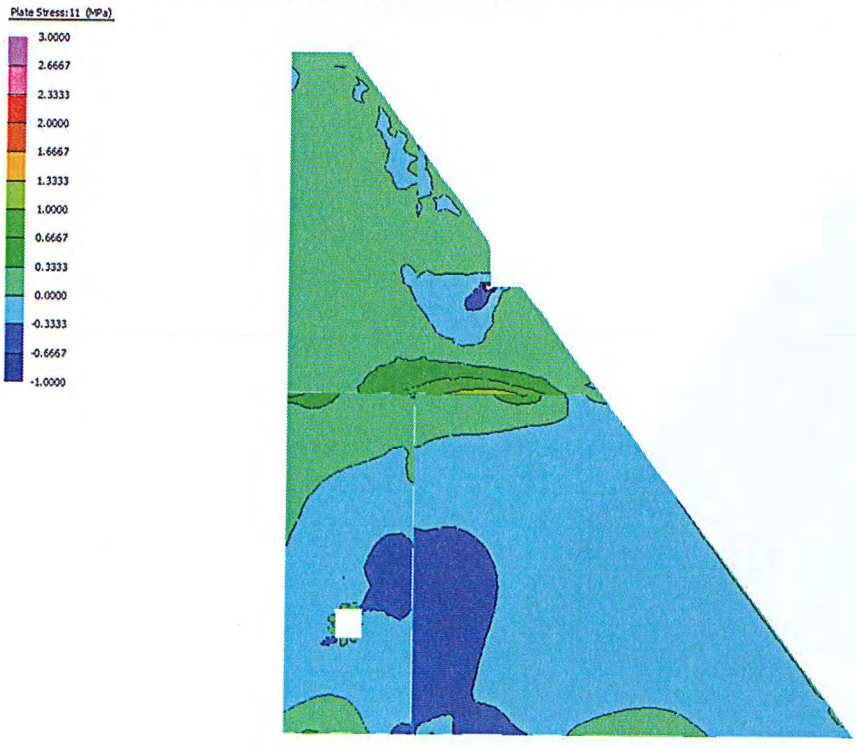

Figure 4.110 SMADRE-4734 – West & Vertical Components – Maximum Opening of Horizontal Crack at U/S Face (4.98s) – Maximum Principal Stress Direction

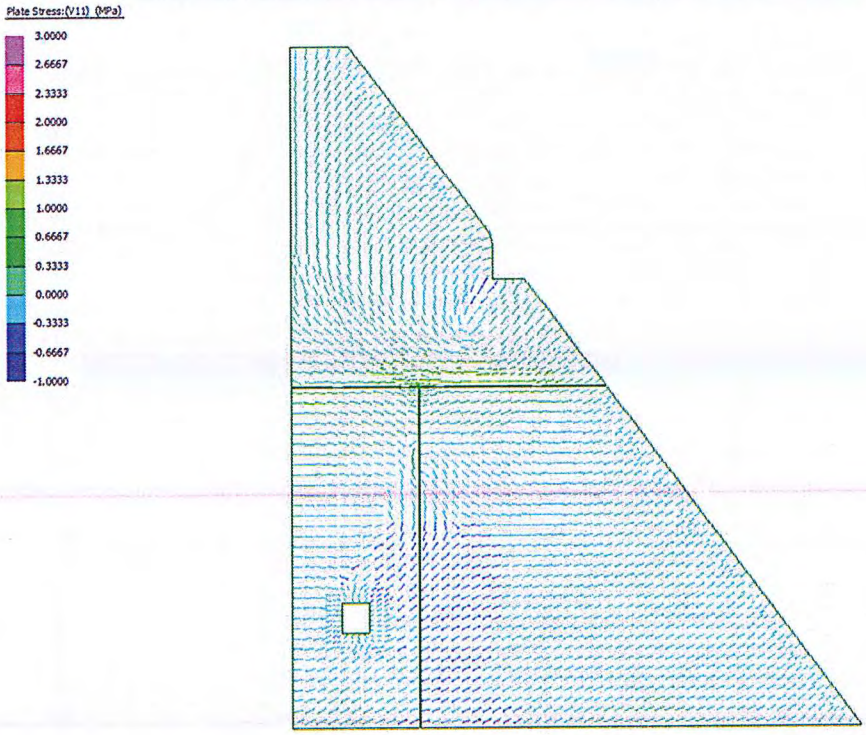

4.6.2 Displacement charts

Figure 4.111 NORTH529 – East & Vertical Components – Base Residual Horizontal Displacement

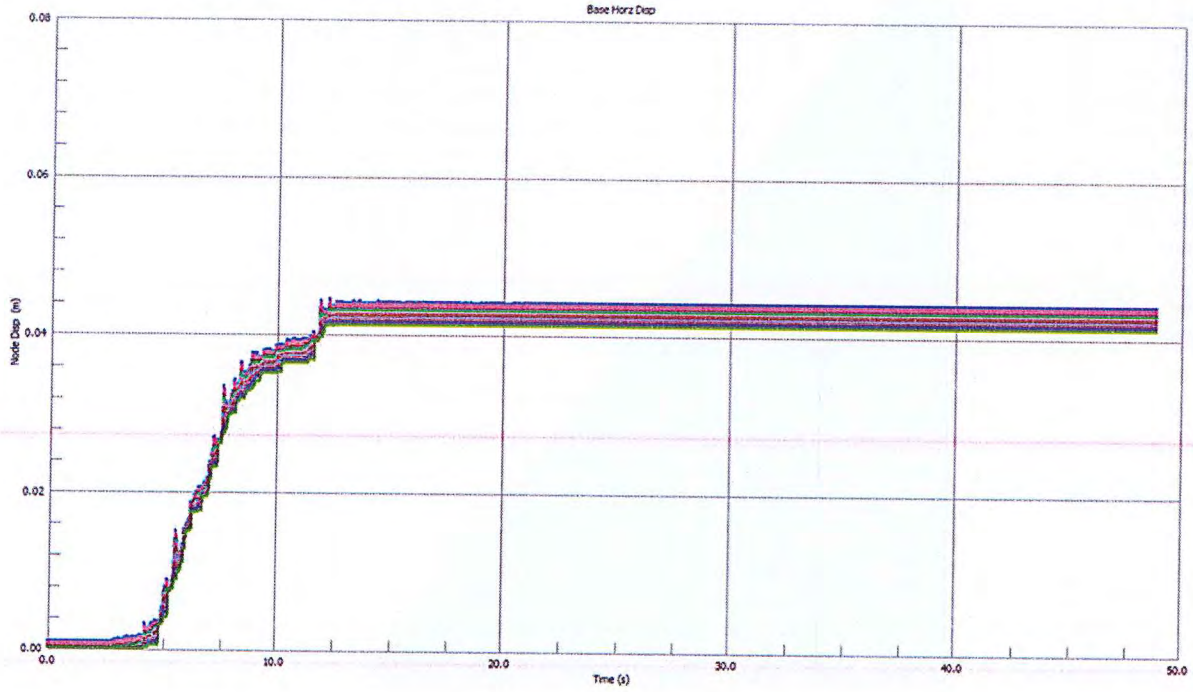

Figure 4.112 NORTH529 – East & Vertical Components – Vertical Crack Horizontal Displacement

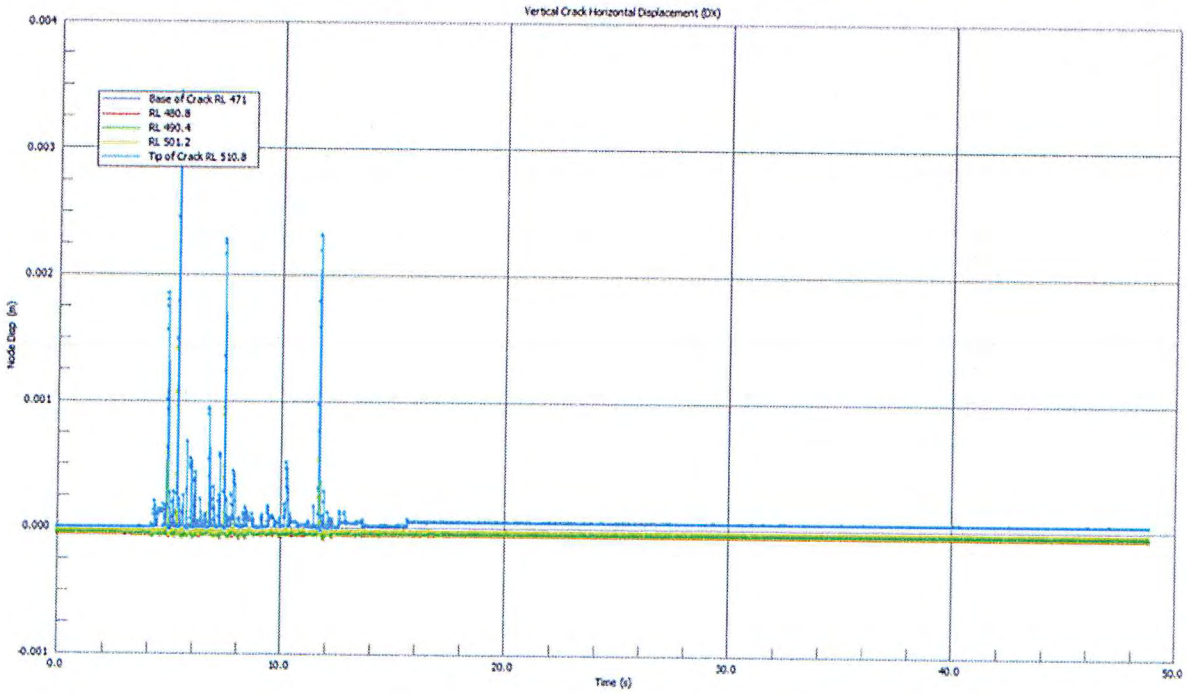

Figure 4.113 NORTH529 – East & Vertical Components – Vertical Crack Vertical Displacement

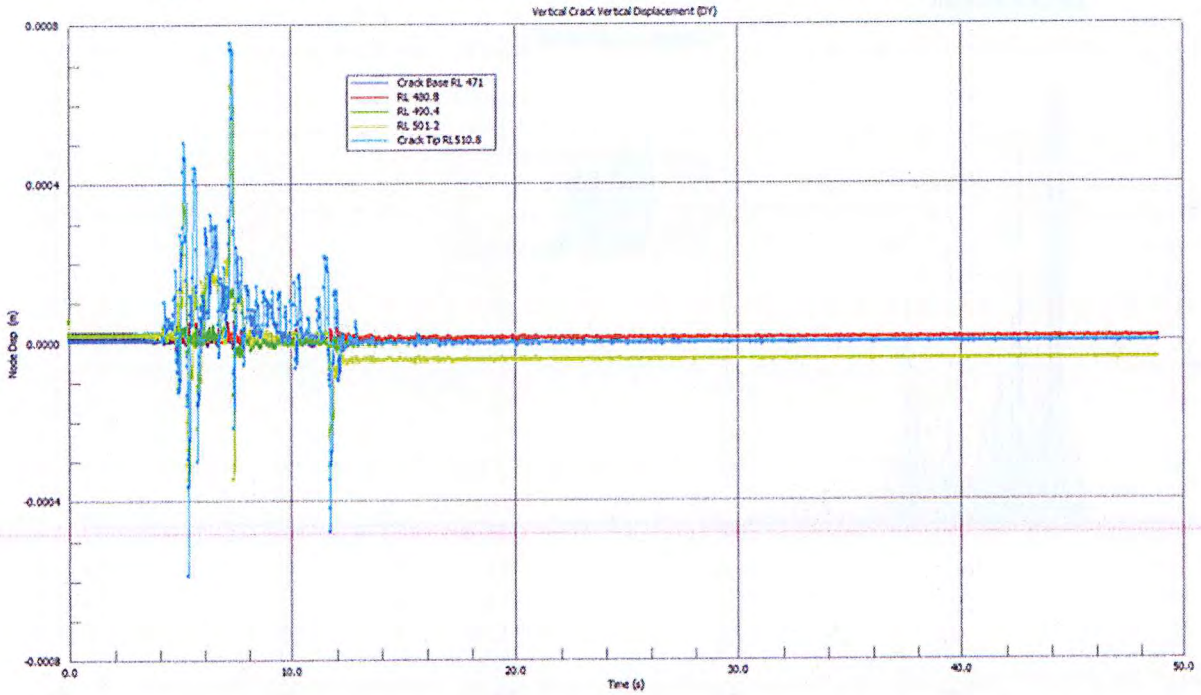

Figure 4.114 NORTH529 – East & Vertical Components – Horizontal Crack Horizontal Displacement

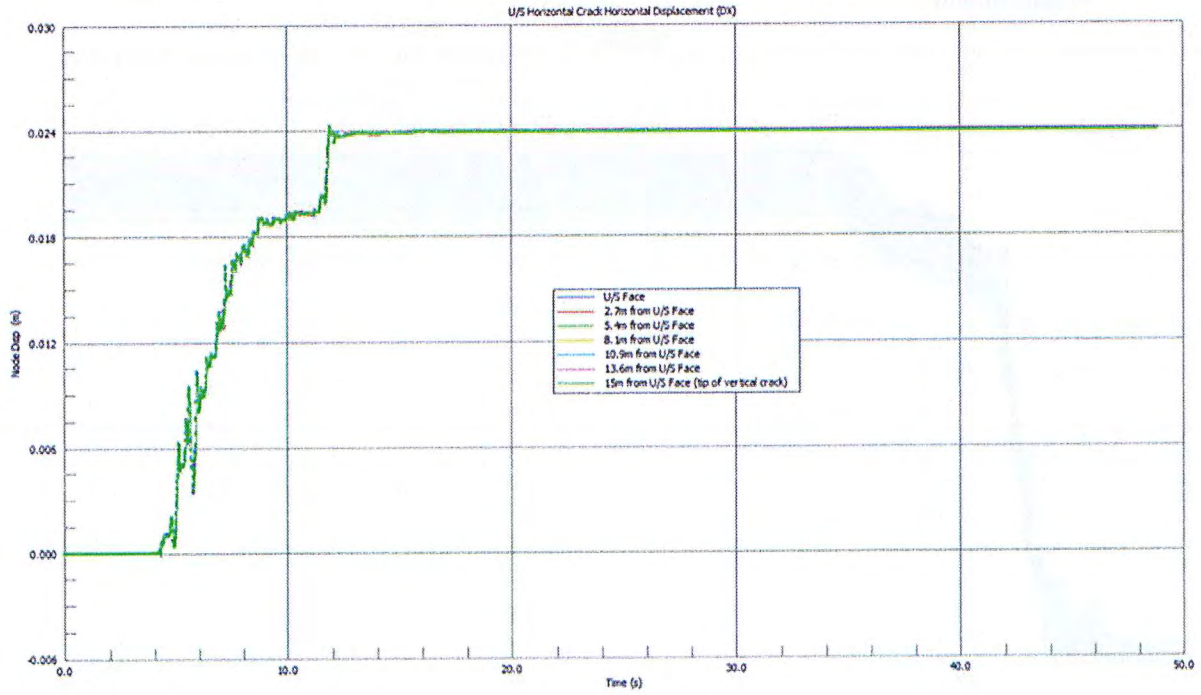

Figure 4.115 NORTH529 – East & Vertical Components – Horizontal Crack Vertical Displacement

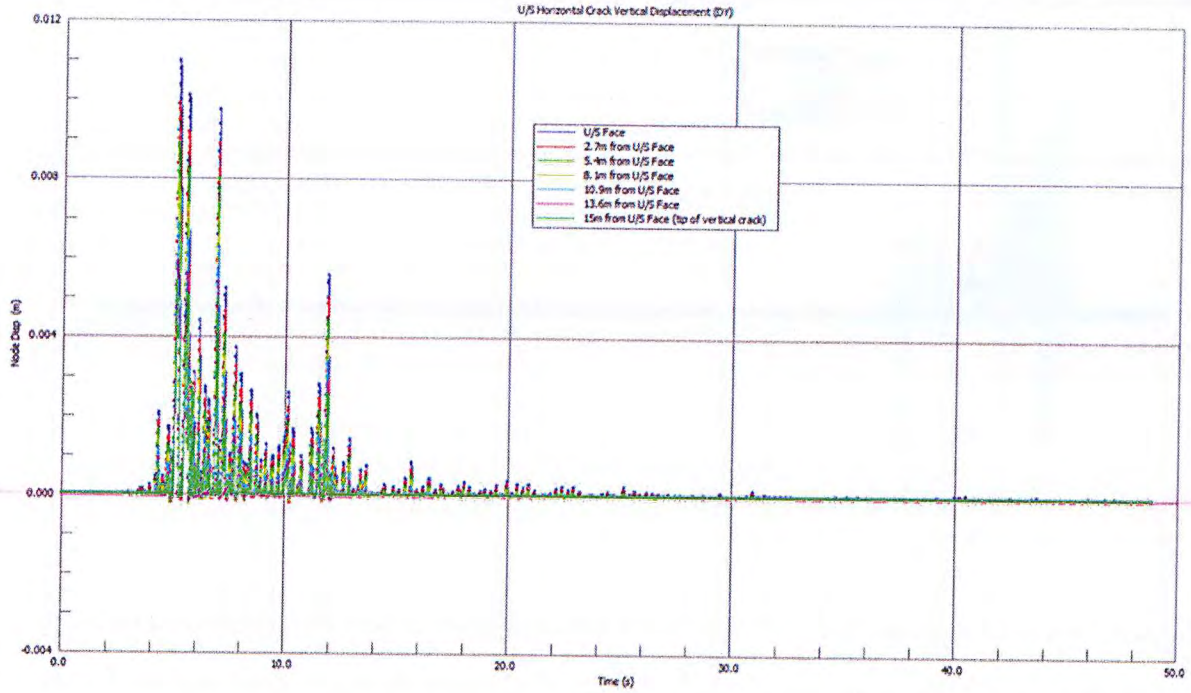

Figure 4.116 NORTH529 – North & Vertical Components – Base Residual Horizontal Displacement

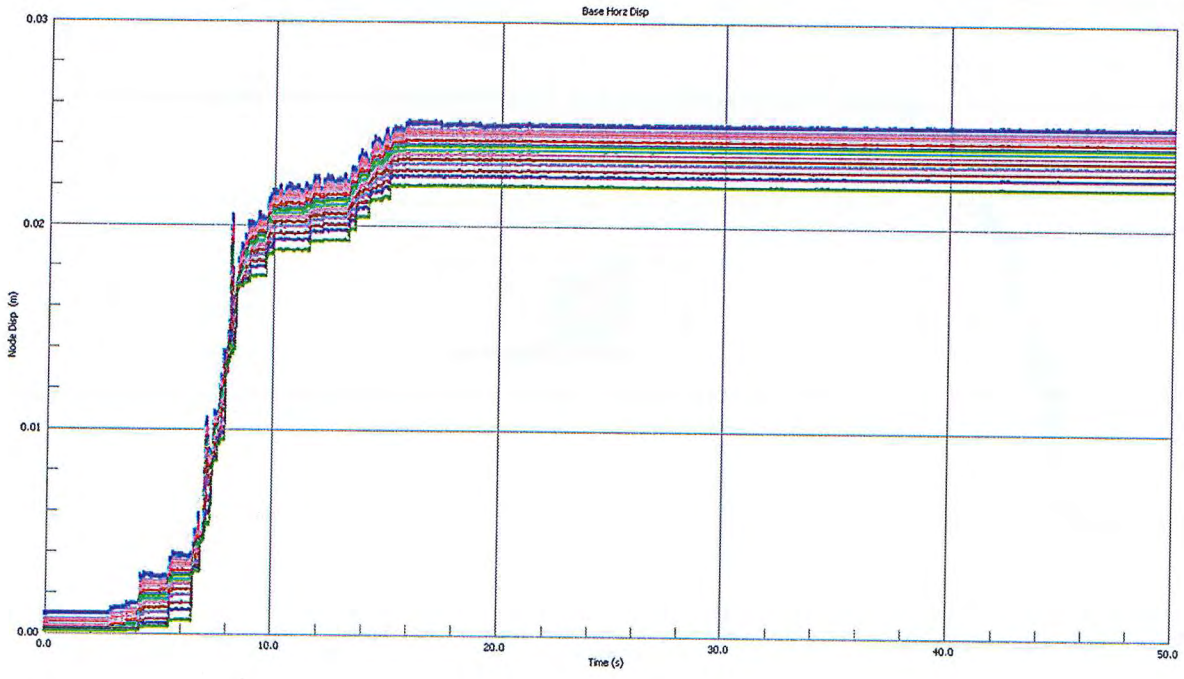

Figure 4.117 NORTH529 – North & Vertical Components – Vertical Crack Horizontal Displacement

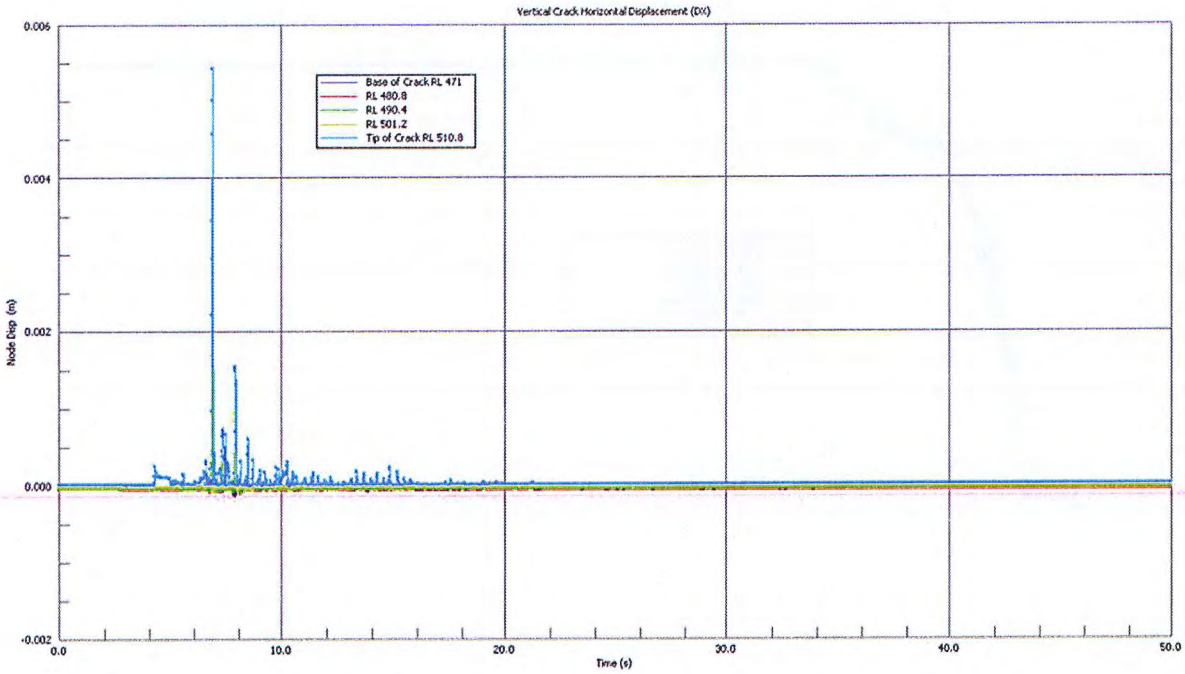

Figure 4.118 NORTH529 – North & Vertical Components – Vertical Crack Vertical Displacement

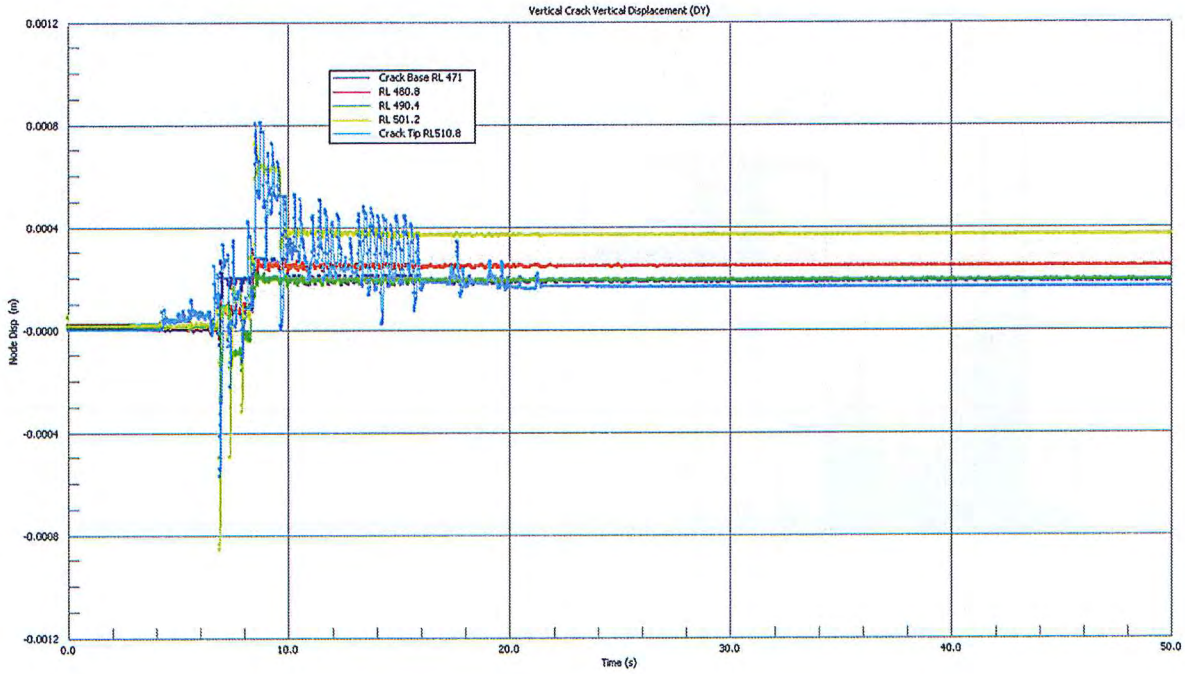

Figure 4.119 NORTH529 – North & Vertical Components – Horizontal Crack Horizontal Displacement

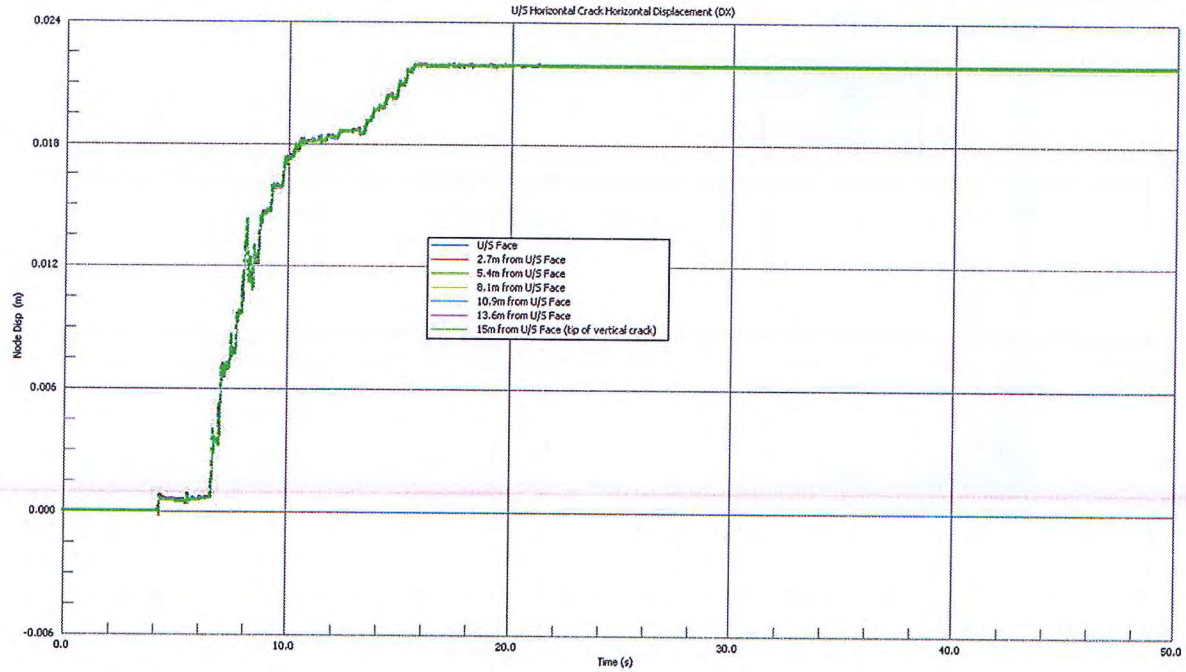

Figure 4.120 NORTH529 – North & Vertical Components – Horizontal Crack Vertical Displacement

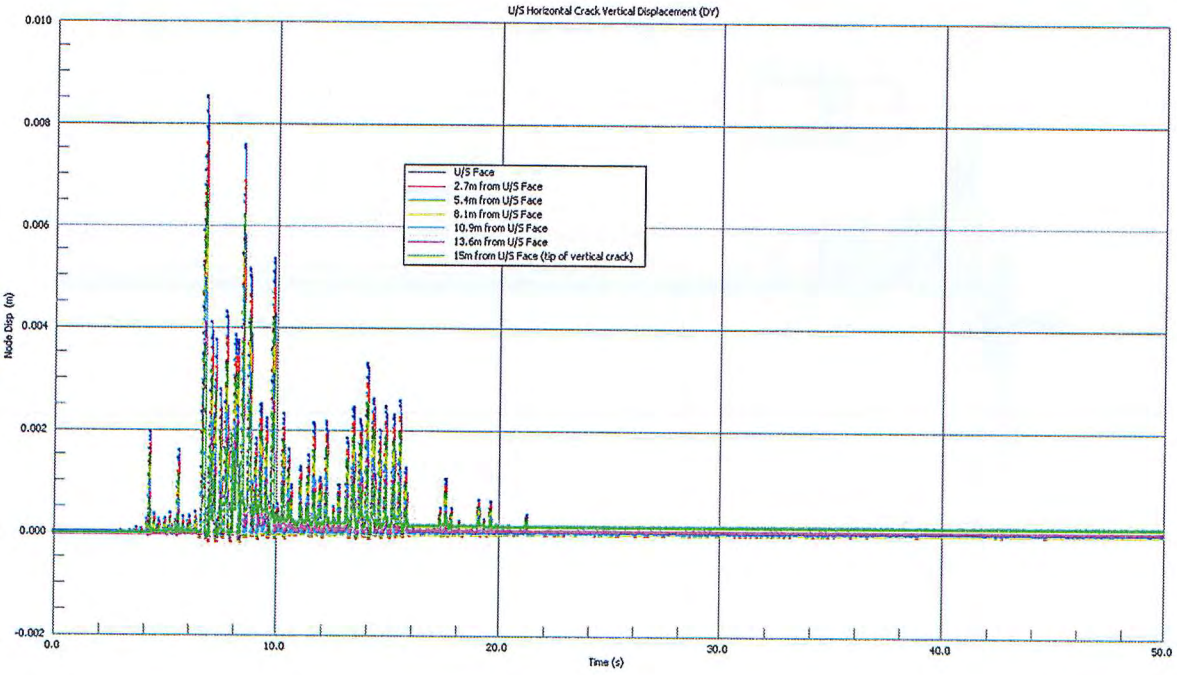

Figure 4.121 NORTH-WON – South & Vertical Components – Base Residual Horizontal Displacement

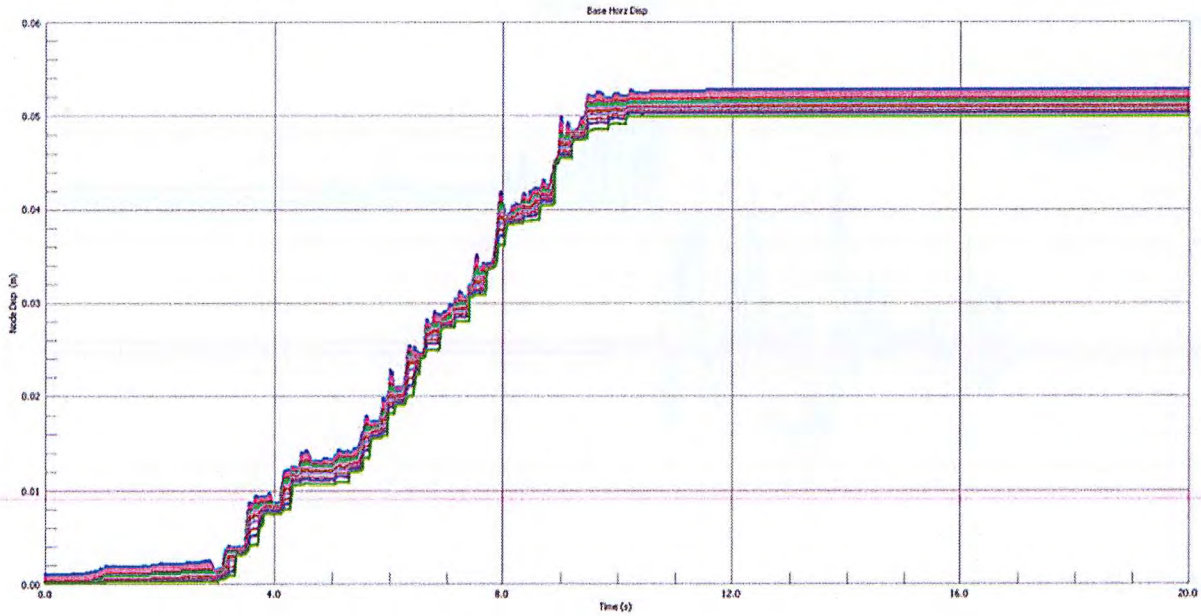

Figure 4.122 NORTH-WON – South & Vertical Components – Vertical Crack Horizontal Displacement

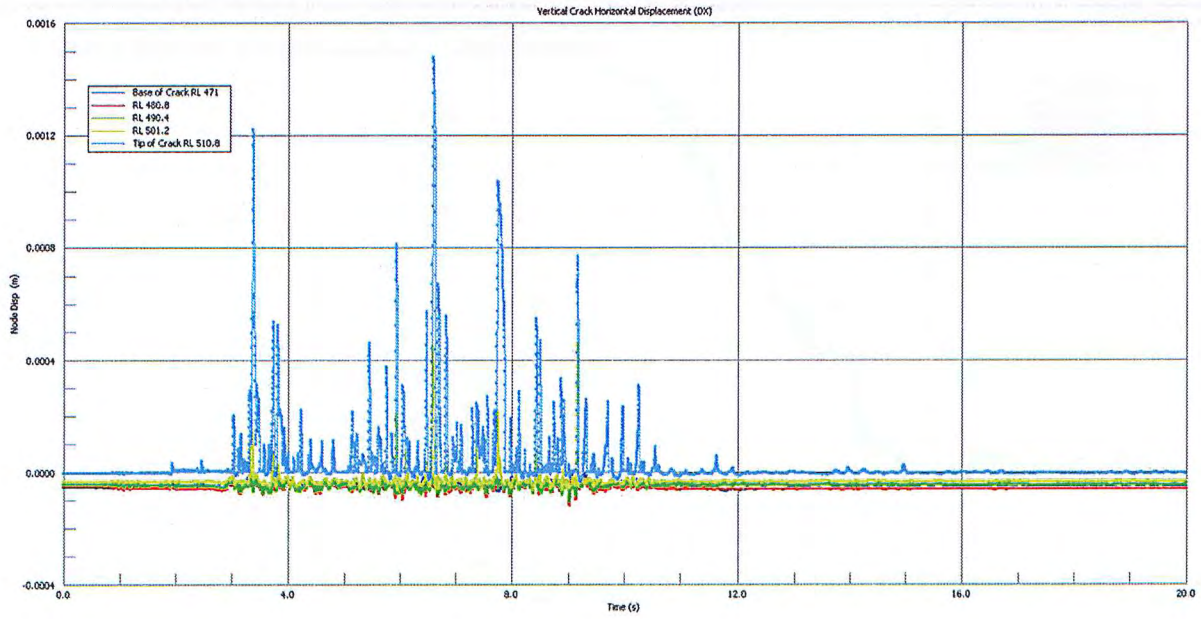

Figure 4.123 NORTH-WON – South & Vertical Components – Vertical Crack Vertical Displacement

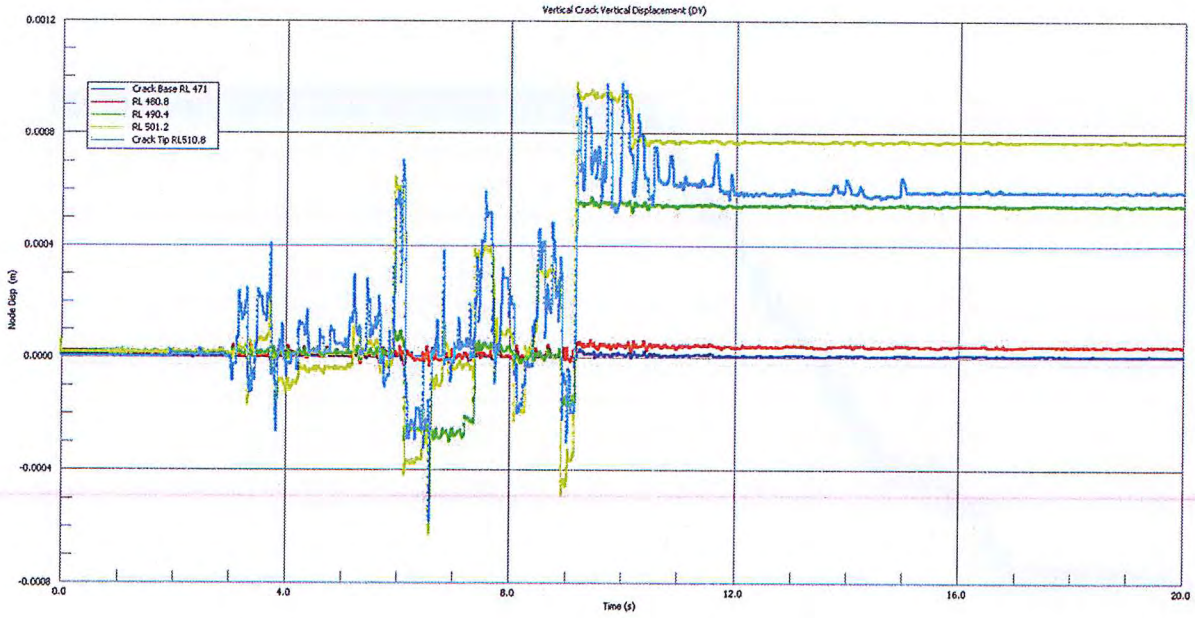

Figure 4.124 NORTH-WON – South & Vertical Components – Horizontal Crack Horizontal Displacement

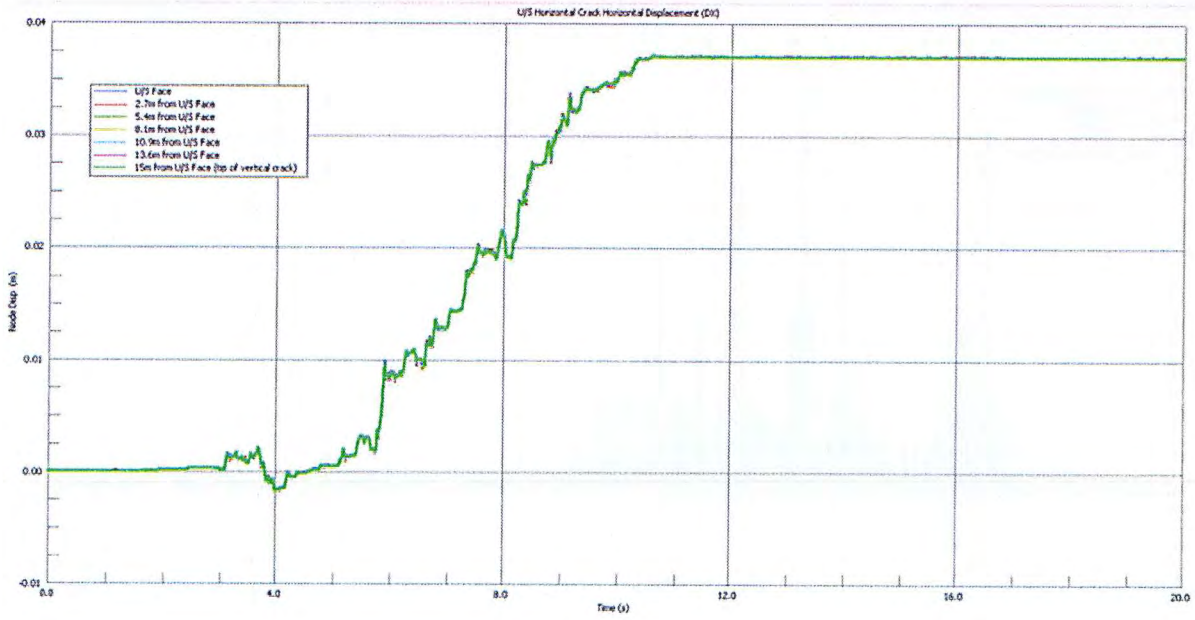

Figure 4.125 NORTH-WON – South & Vertical Components – Horizontal Crack Vertical Displacement

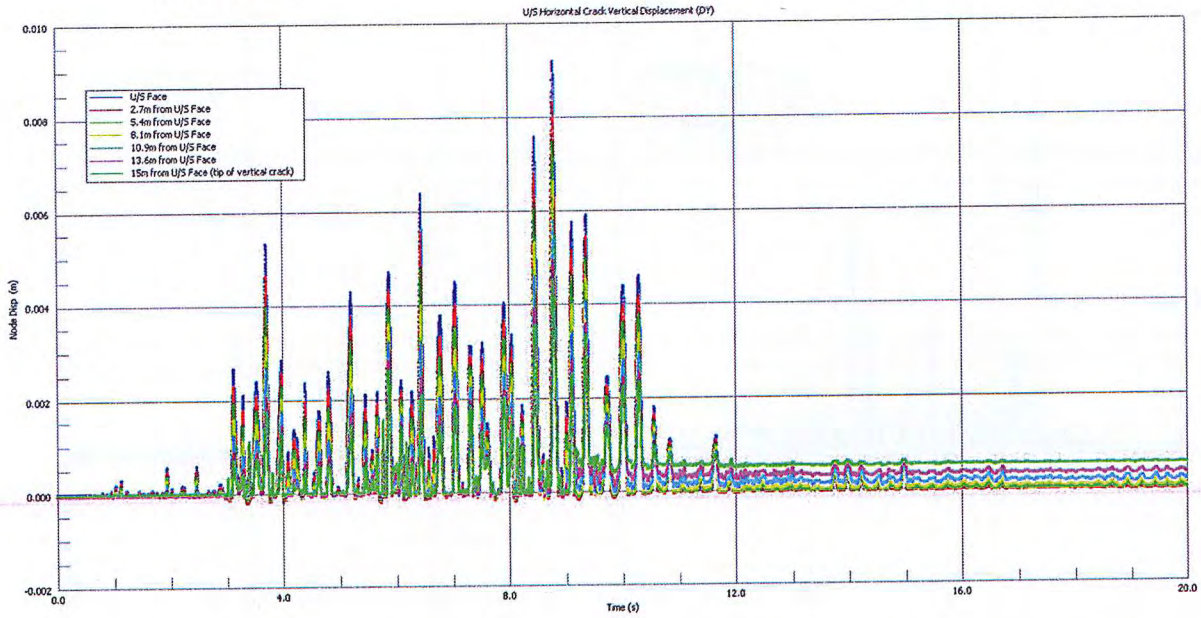

Figure 4.126 NORTH-WON – West & Vertical Components – Base Residual Horizontal Displacement

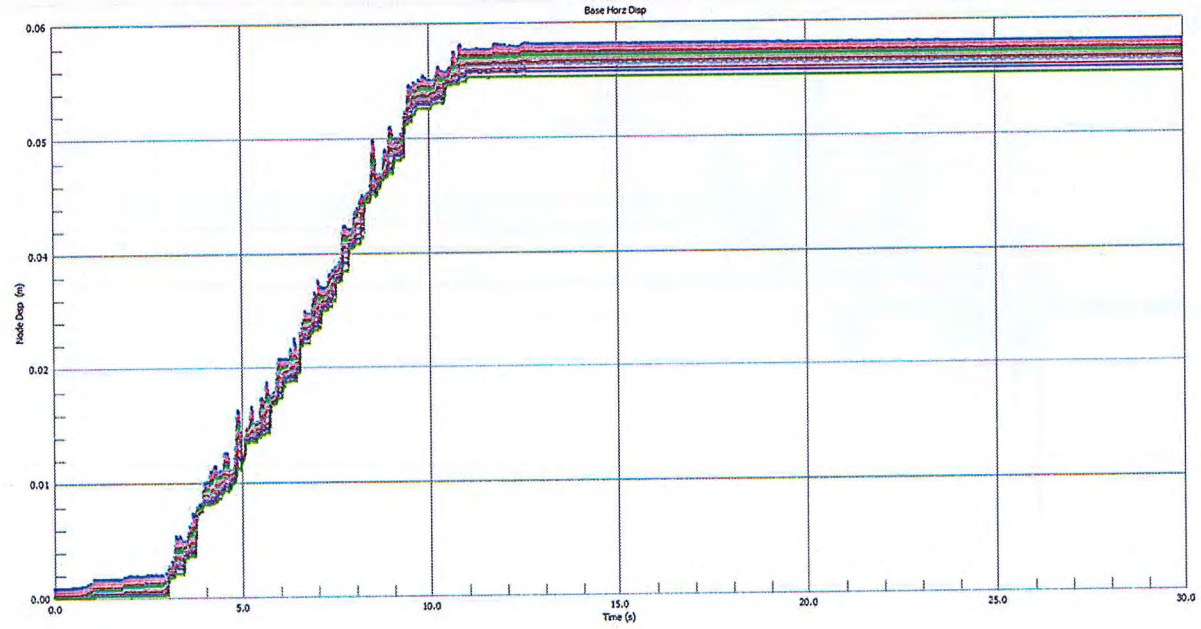

Figure 4.127 NORTH-WON – West & Vertical Components – Vertical Crack Horizontal Displacement

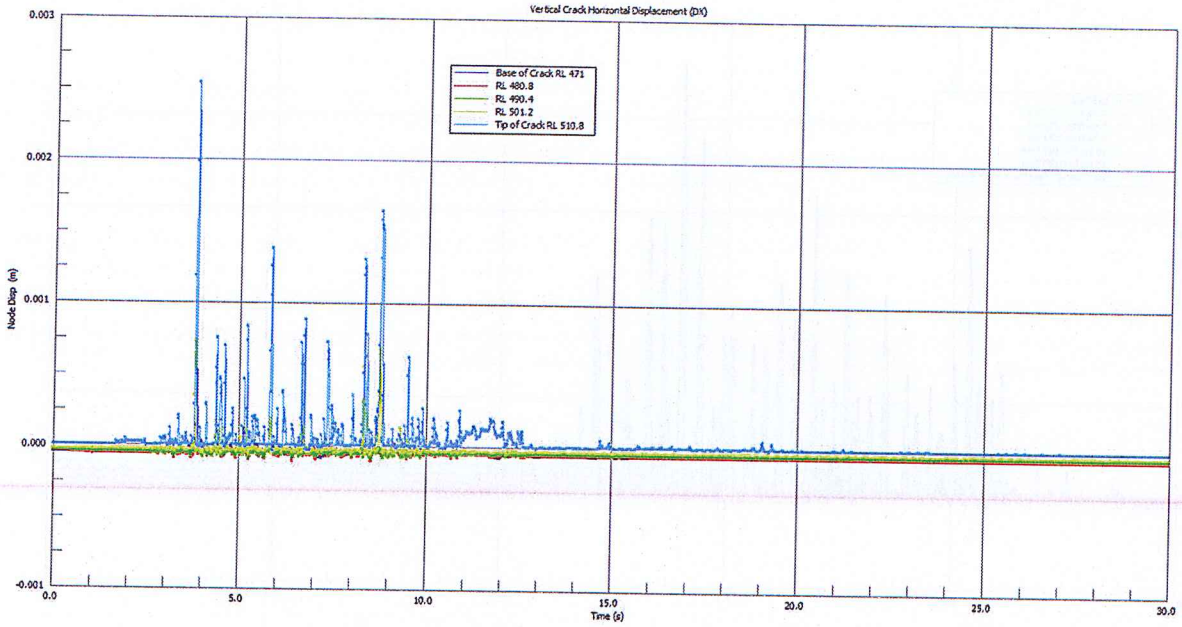

Figure 4.128 NORTH-WON – West & Vertical Components – Vertical Crack Vertical Displacement

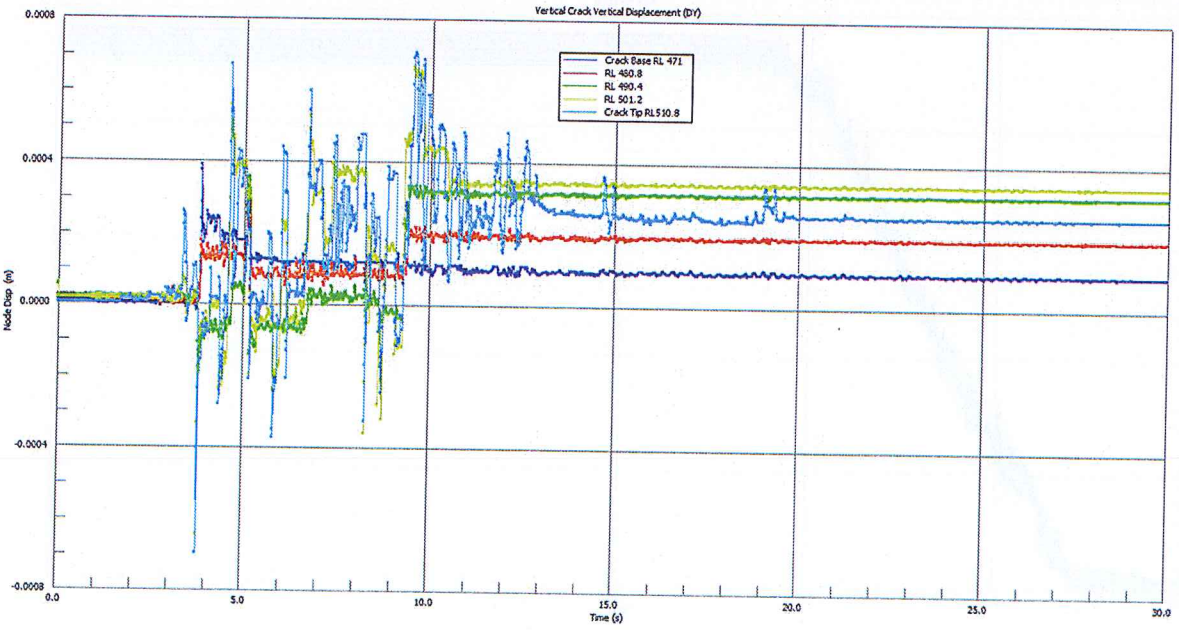

Figure 4.129 NORTH-WON – West & Vertical Components – Horizontal Crack Horizontal Displacement

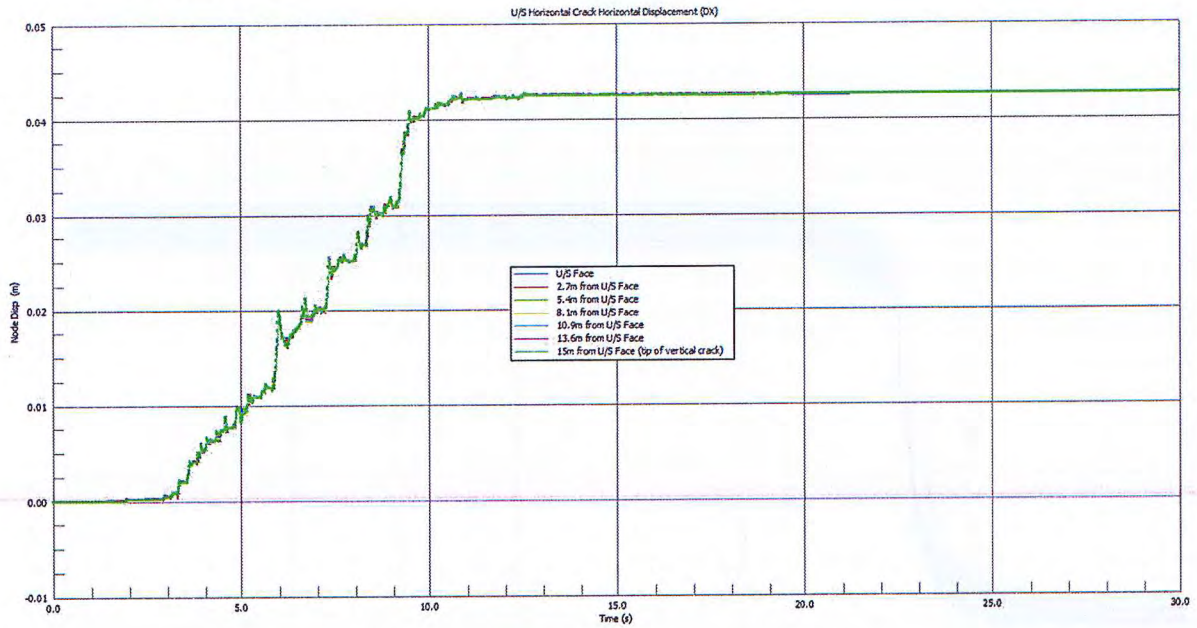

Figure 4.130 NORTH-WON – West & Vertical Components – Horizontal Crack Vertical Displacement

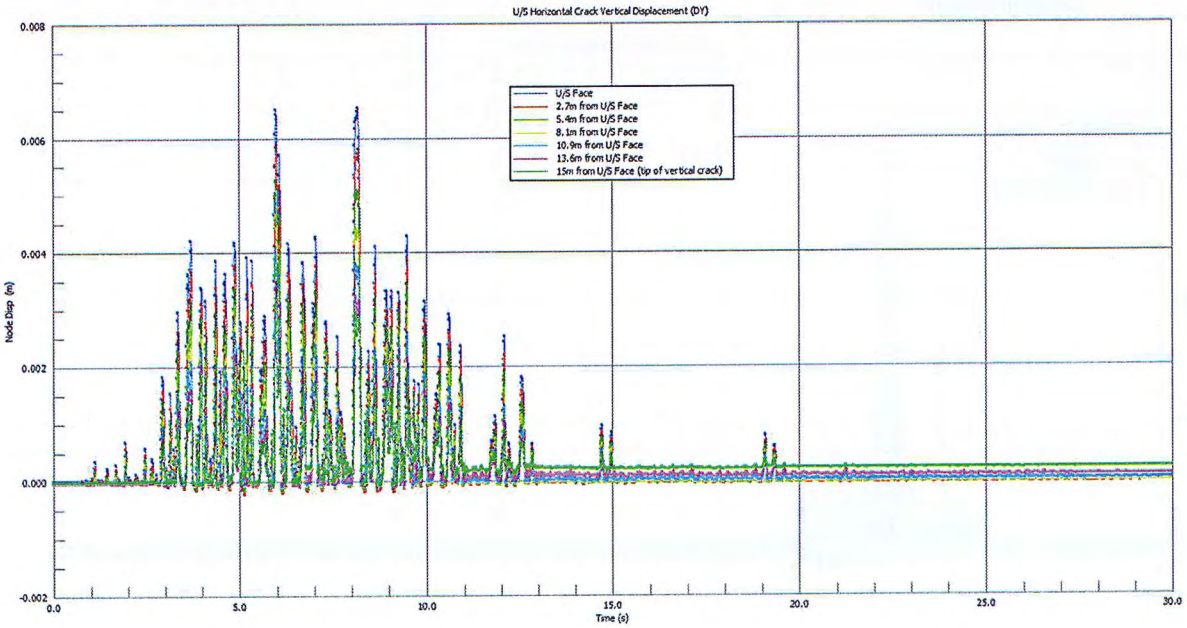

Figure 4.131 SMADRE-4734 – North & Vertical Components – Base Residual Horizontal Displacement

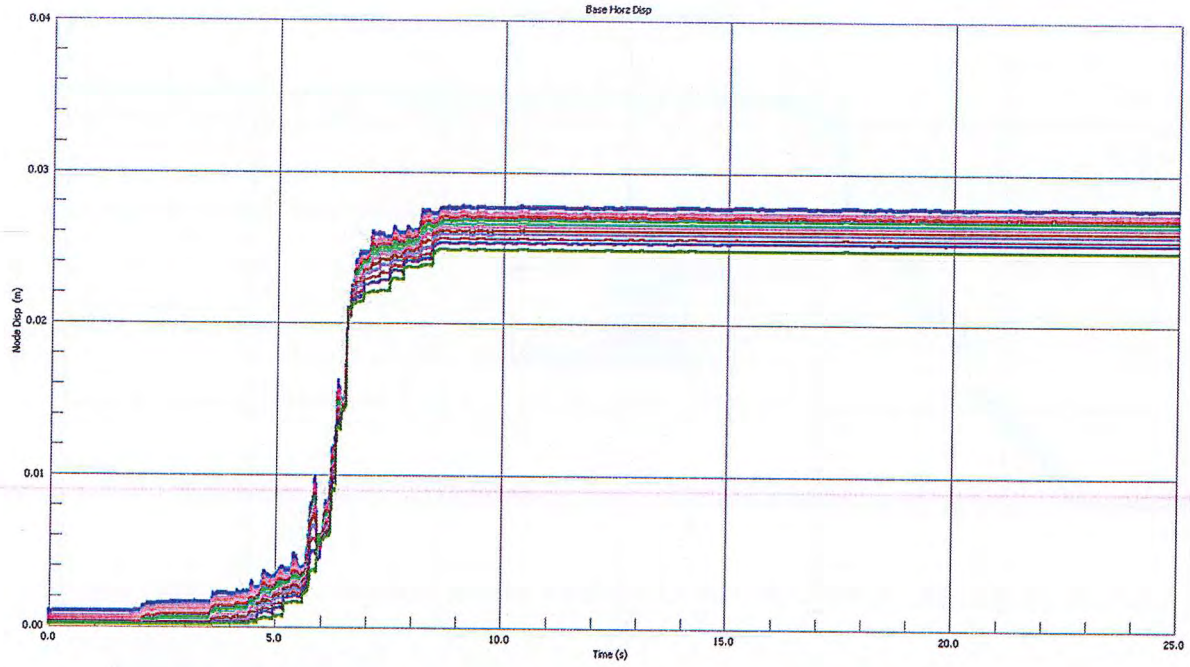

Figure 4.132 SMADRE-4734 – North & Vertical Components – Vertical Crack Horizontal Displacement

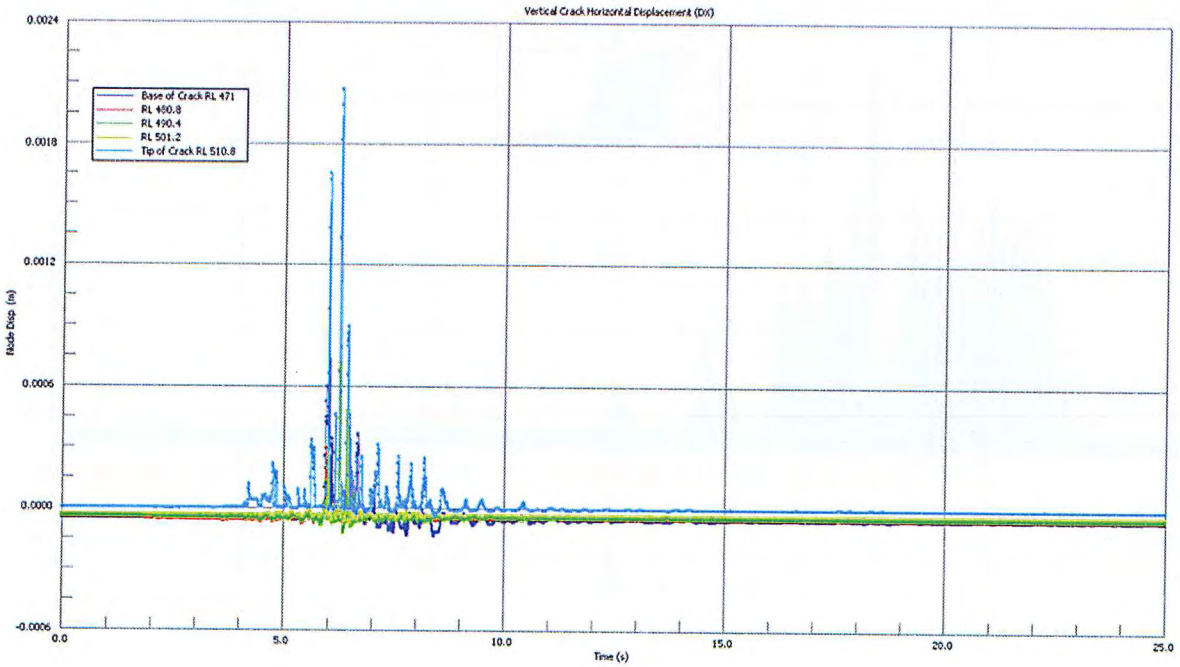

Figure 4.133 SMADRE-4734 – North & Vertical Components – Vertical Crack Vertical Displacement

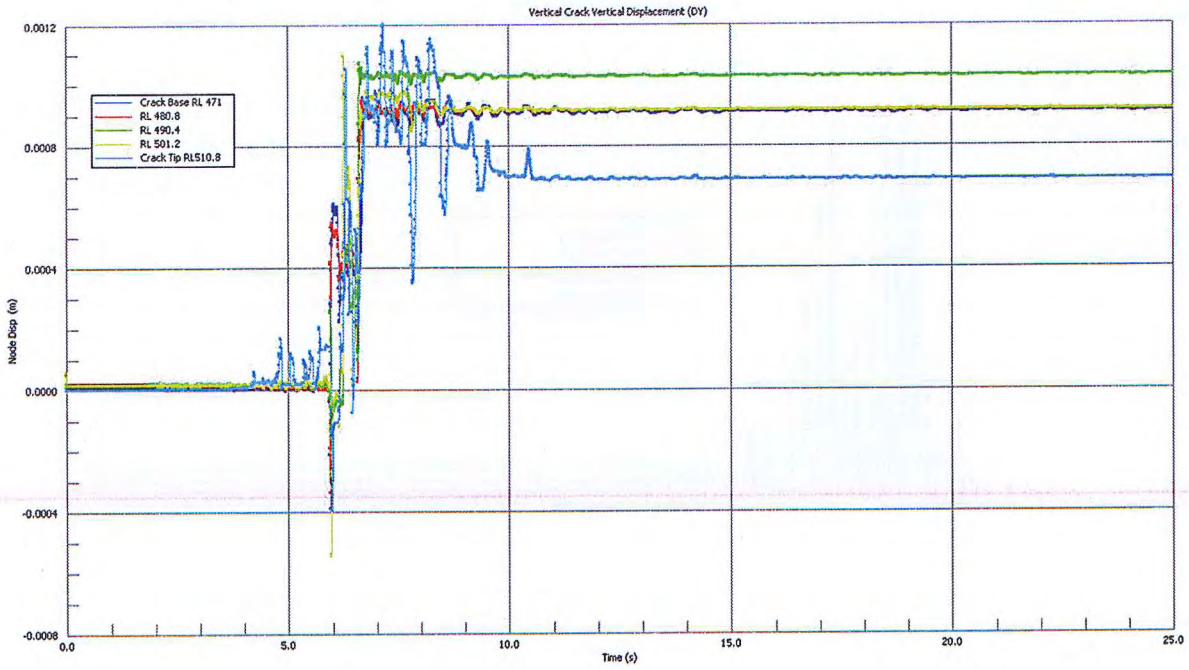

Figure 4.134 SMADRE-4734 – North & Vertical Components – Horizontal Crack Horizontal Displacement

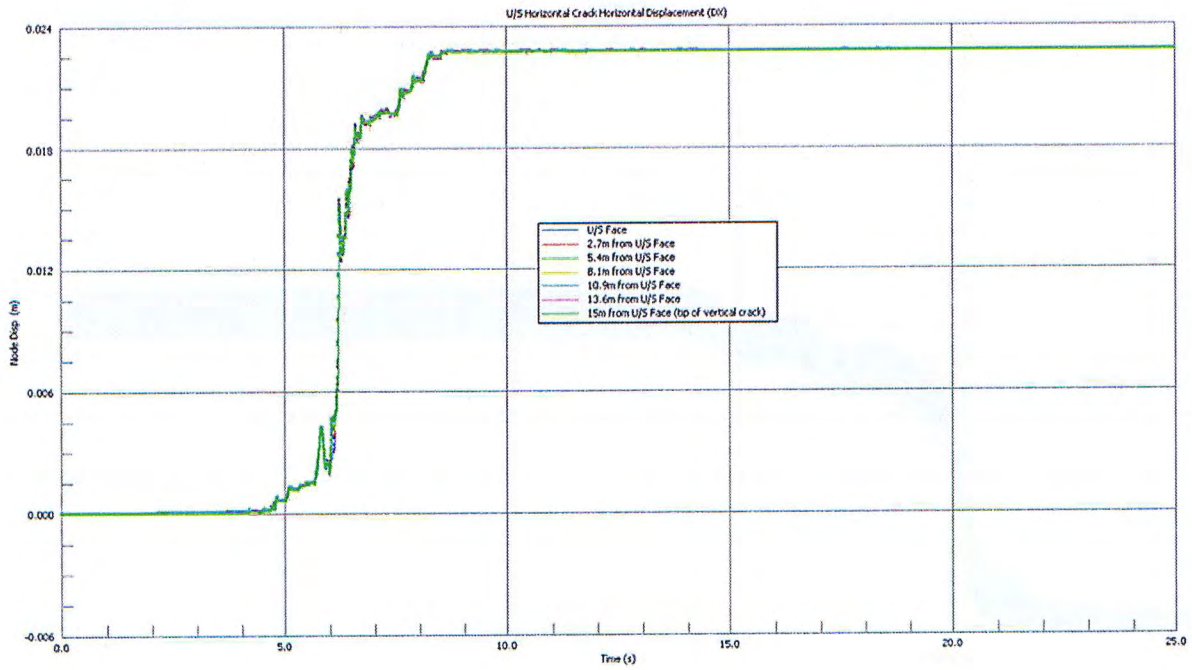

Figure 4.135 SMADRE-4734 – North & Vertical Components – Horizontal Crack Vertical Displacement

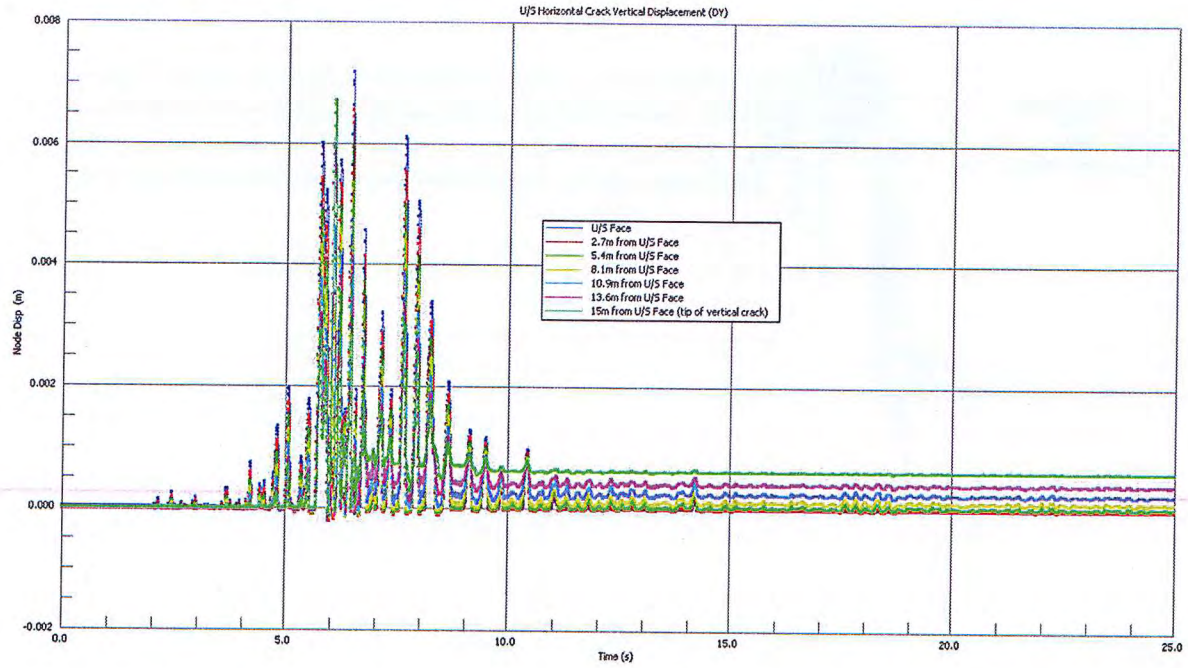

Figure 4.136 SMADRE-4734 – West & Vertical Components – Base Residual Horizontal Displacement

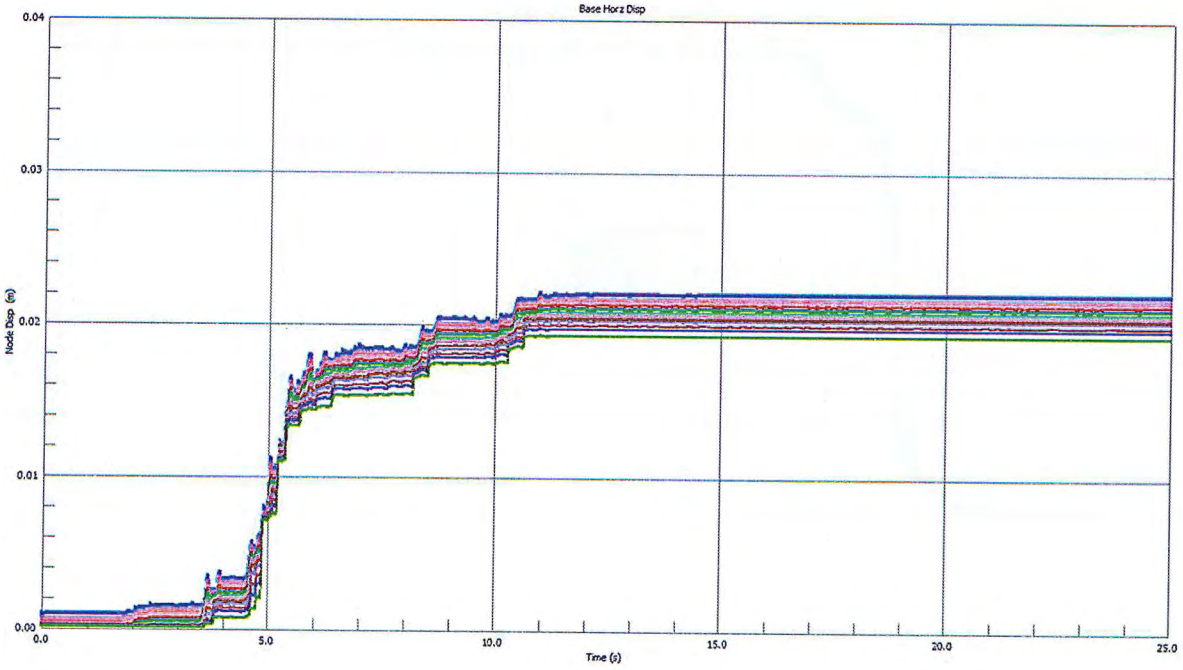

Figure 4.137 SMADRE-4734 – West & Vertical Components – Vertical Crack Horizontal Displacement

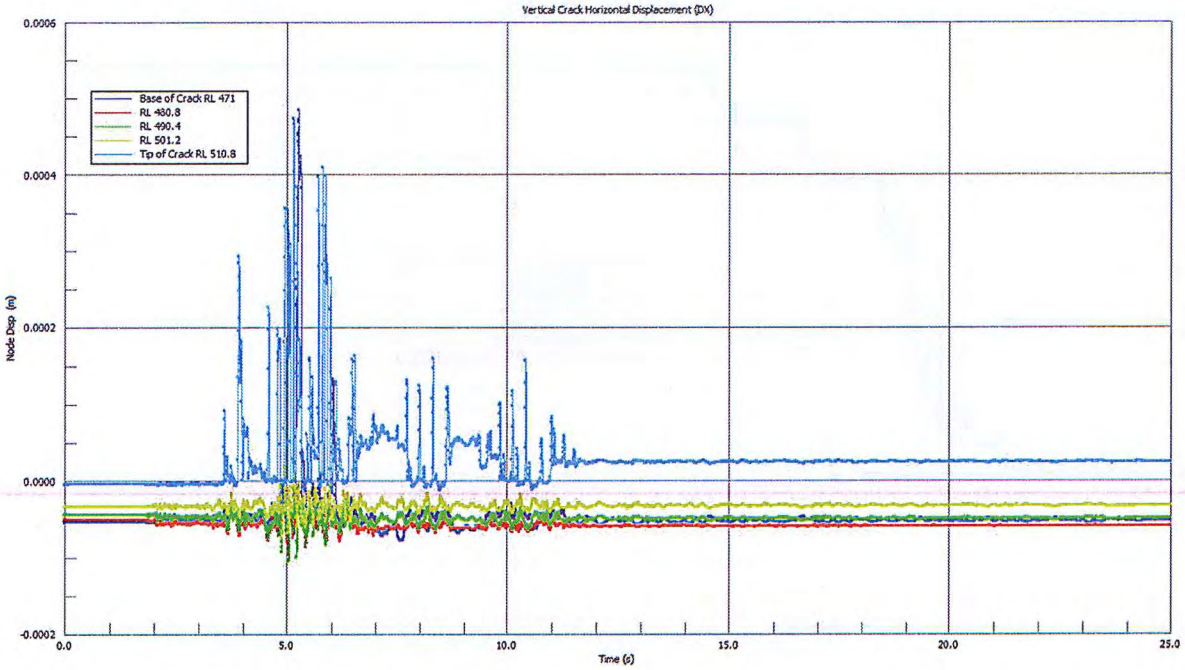

Figure 4.138 SMADRE-4734 – West & Vertical Components – Vertical Crack Vertical Displacement

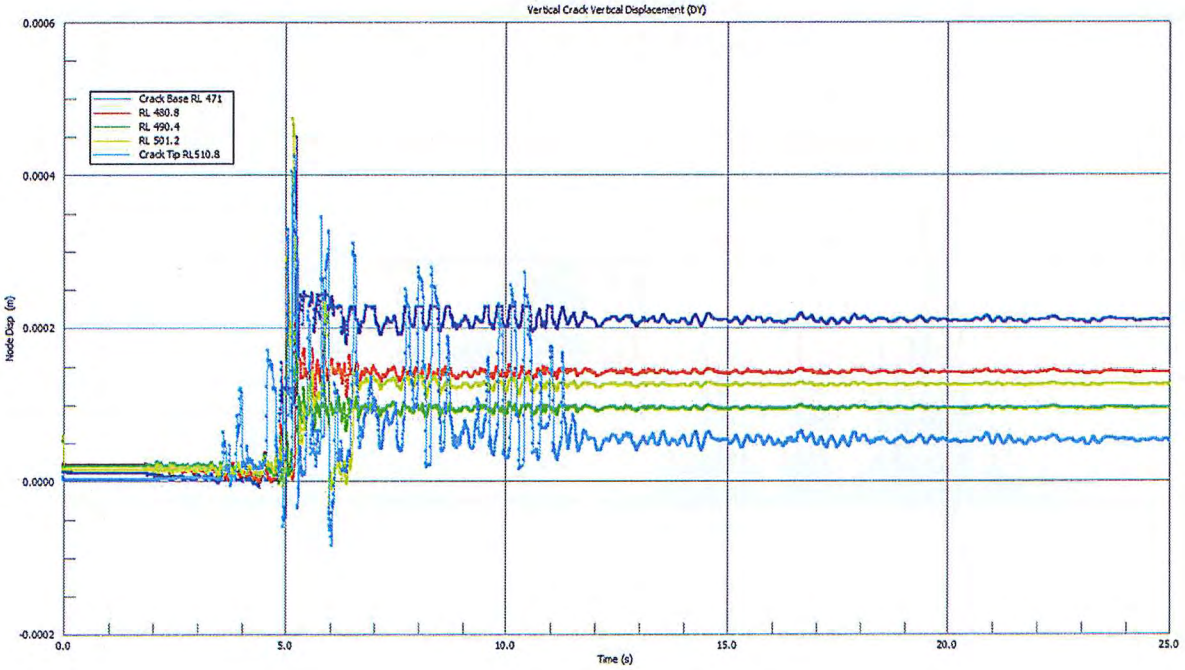

Figure 4.139 SMADRE-4734 – West & Vertical Components – Horizontal Crack Horizontal Displacement

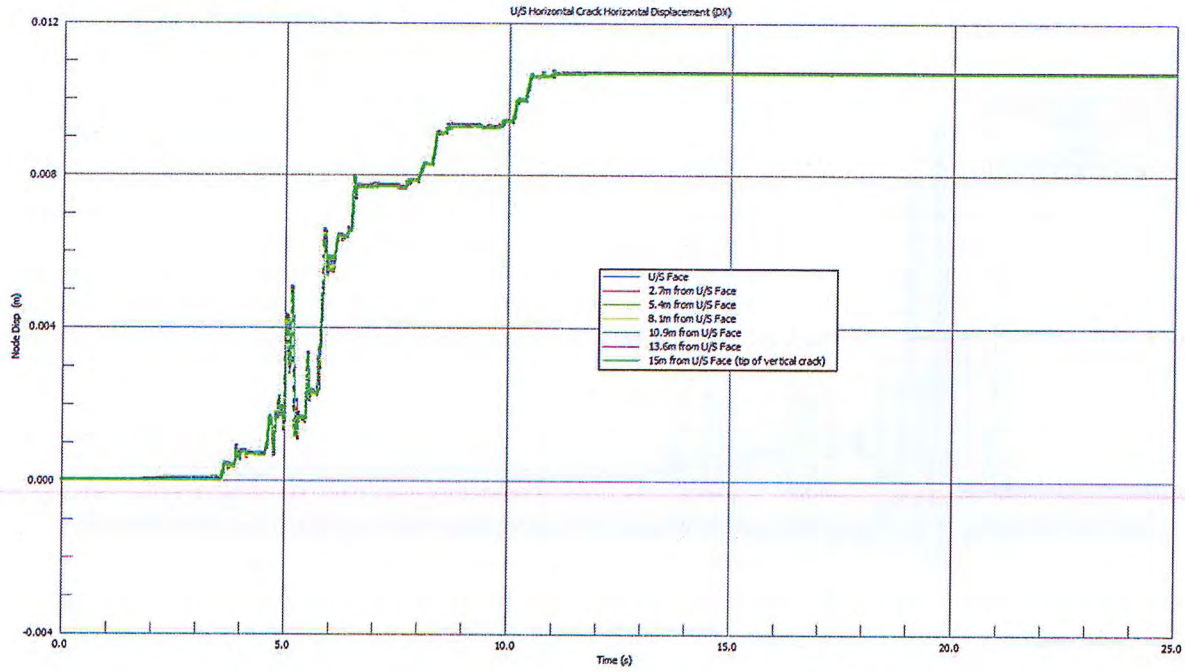

Figure 4.140 SMADRE-4734 – West & Vertical Components – Horizontal Crack Vertical Displacement

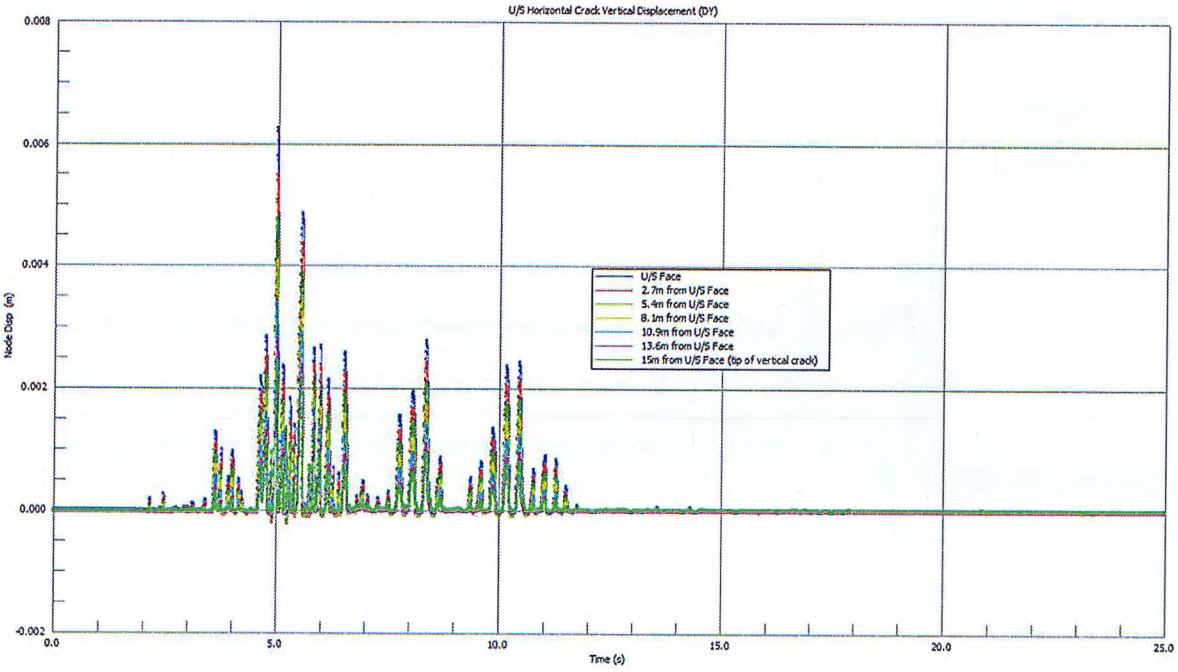

4.6.3 Discussion – Non Linear Analysis

From the stress envelope plots from the non-linear analysis (refer Figure 4.87 to Figure 4.110) it can be seen that the inclusion of the horizontal crack has reduced the magnitude of stresses produce by seismic loading. This is with the exception of the increase stresses observed along the horizontal crack as a result of downstream movement of the upper section of the dam (11 mm to 42 mm). This displacement of the upper section of the dam, should it occur, would be significant and as such would likely result in some emergency actions being put in place (ie the reservoir being drawn down). However it is small in comparison with the frictional contact area along the crack and as such it would be expected to have only a negligible effect on the post seismic stability of the dam. Downstream displacement is also observed at the dam foundation (ranging from approximately 22 mm to 58 mm). This is less than previously seen in the uncracked model. This reduced displacement is due to the additional energy dissipation provided by the horizontal crack.

The relative opening of both horizontal and vertical crack (refer Figure 4.111 to Figure 4.140) is also typically less than 1 mm. Such a small opening of the cracks during the seismic event should not be sufficient to reduce the frictional resistance across the crack surface particularly due to the size of the aggregate used in the RCC as well as undulations in the lift joints. However the limitations of the current model are such that any opening of the crack does not allow for friction resistance across the non-linear elements. As a result it would be expected that displacements of the upper portion of the dam and at the dam foundation interface would be smaller than what has been observed in the non-linear models.

4.7 Combined Thermal and Seismic Loading

The seismic analyses discussed in the preceding sections do not consider the thermal stresses that would have developed within the body of the dam. These should be included in the analysis to provide the total stresses that the dam would experience. The 2031 winter condition has been adopted for the temperature profile as this typical long term condition, with the dam in its most downstream deflected position.

Ideally the temperature profile, and therefore the resulting stresses would be included in a single model. However, this is beyond the capabilities the STRAND7 software.

As an alternative, a simplified approach has been adopted whereby the non-seismic induced stresses from thermal, self-weight and reservoir water loads have been compared with the same model excluding thermal loads to assess whether the long-term thermal stresses have a significant impact on the seismic behaviour of the dam. The assumption is that if the stress distributions for both cases are similar in both magnitude and direction then, when adopted as the t=0 time step condition for the seismic analysis, there will be no significant difference between resulting calculated stresses for the seismic load cases.

Figure 4.141 to Figure 4.143 show the vector plots for the maximum principal stress, the contour plot for the vertical stress and the deflected shape including the thermal loads in the winter of 2031.

Figure 4.144 to Figure 4.146 show vector plots for the maximum principal stress, the contour plot for the vertical stress and the deflected shape, excluding the thermal loads in the winter of 2031.

Above the gallery level the differences in magnitude and direction of the principal stresses and the magnitude of the vertical stresses on the outer faces are not considered to be significant in how they will impact on the stresses calculated in the seismic analysis. Both the models are indicating compressive stresses on both faces of the dam. The model including the thermal loads, is showing higher compressive stresses (> 1 MPa, the limit of the contour range in the plot), whereas the model excluding the thermal loads shows the compressive stresses in the range of 0 to 1MPa. However, towards the centre of the dam the thermal model is showing small tensions (up to 0.8MPa) where as the model excluding the thermal loads remains in compression for the full width of the section.

Therefore it can be concluded that if the thermal loads had been included in the seismic model, these thermal stresses, when combined with the seismic stresses, would have produced more compressive vertical stresses on the outer parts of the dam and higher tensile stresses within the body of the dam. As such it would be expected that, given the higher compressive stress on the outer faces, the initiation of cracking would be delayed when compared to the seismic models analysed (refer to Section 4.3.3). However, once cracking initiated, it would likely propagate deeper into the centre of the section, due to the higher tensile stresses within the body of the dam. This level of assessment is beyond the capability of the STRAND7 software, and therefore the model adopted for the non-linear analysis (ie a full width crack at RL 511.3m AHD) would still be representative of the "cracked dam" model.

Below the gallery level there is significant difference in the magnitude and direction of the stresses. The thermal model develops high tensile stresses due to the restraint of the foundation as the concrete cools. This does not occur in the model excluding the thermal loading. Although this will have an impact on the calculated stresses in the seismic analysis, it is not considered to be significant as the differential movement and therefore induced stresses calculated in the seismic model are generally low in the area below the gallery (typically less than 0.5MPa). Therefore the thermal stress will dominate in this area and as previously shown, the thermal stresses do not exceed the allowable stress. In those areas where the seismic induced stresses are of a greater magnitude, they tend to be limited in extent (eg refer Figure 4.103)..

Therefore it can be concluded that although the inclusion of the thermal loads in the seismic analysis would provide a more accurate assessment of the stresses developed during a seismic event, the impact of excluding the thermal loads has no material influence on the calculated stresses discussed in this Report.

Figure 4.141 Maximum Principal Stress - Winter 2031 - Thermal Load Included

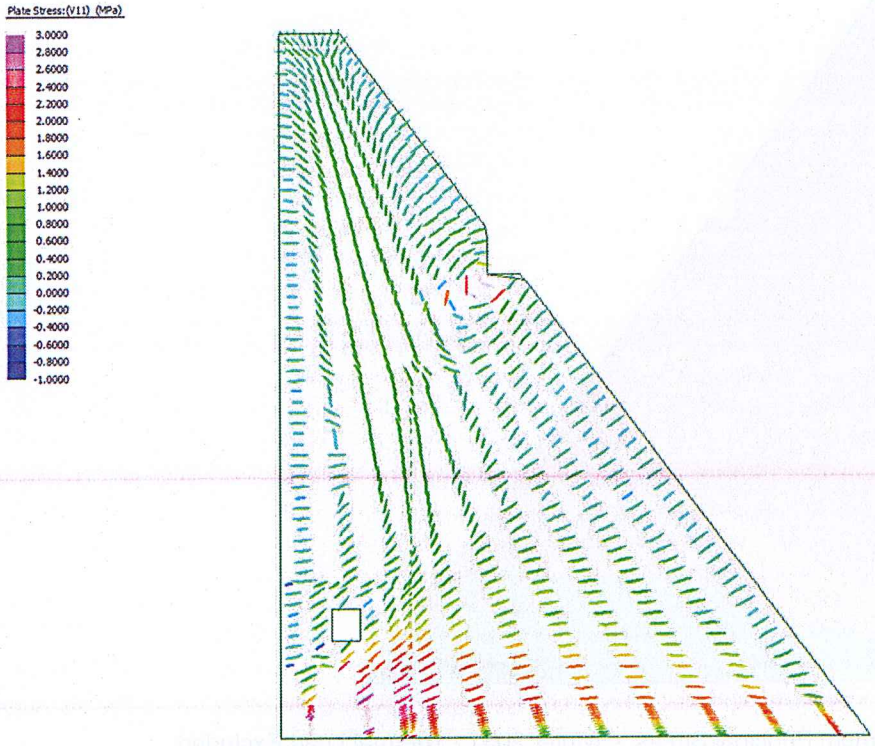

Figure 4.142 Vertical Stress - Winter 2031 – Thermal Loads Included

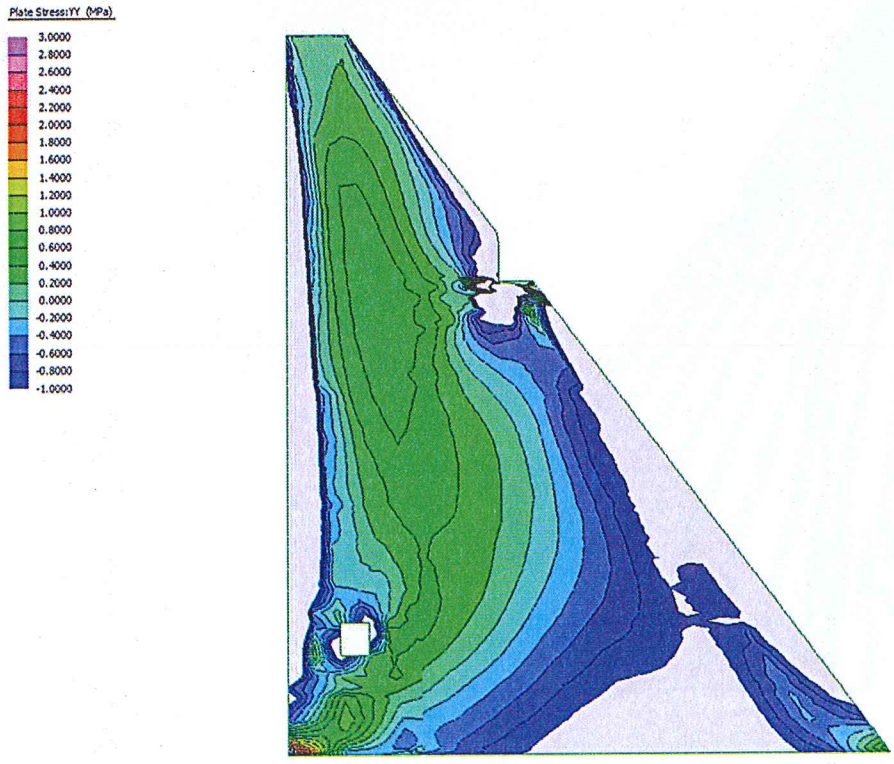

Figure 4.143 Deflected Shape - Winter 2031 -Thermal Load Included

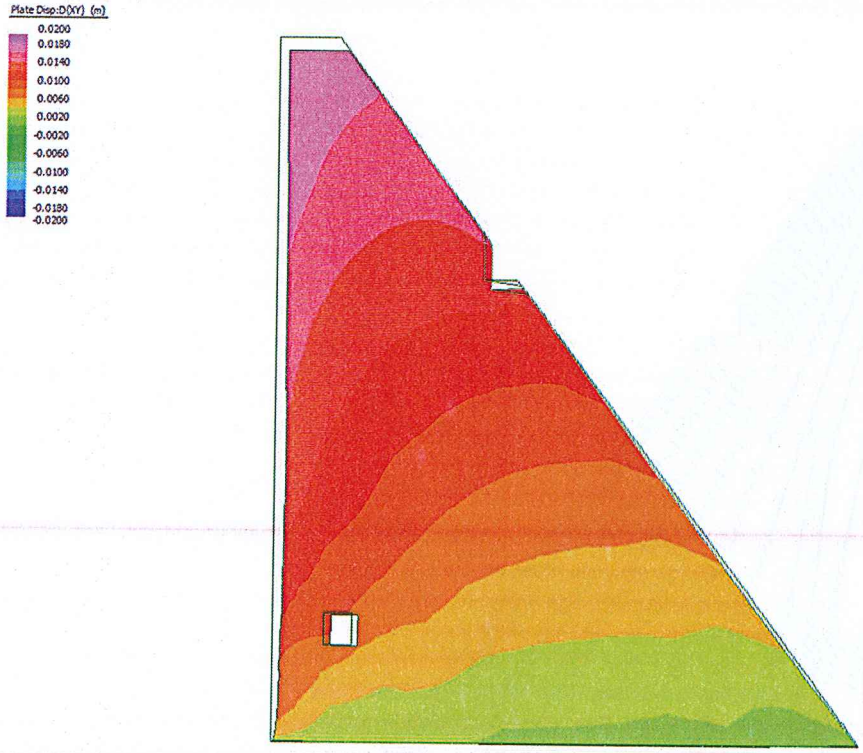

Figure 4.144 Maximum Principal Stress - Winter 2031 - Thermal Load Excluded

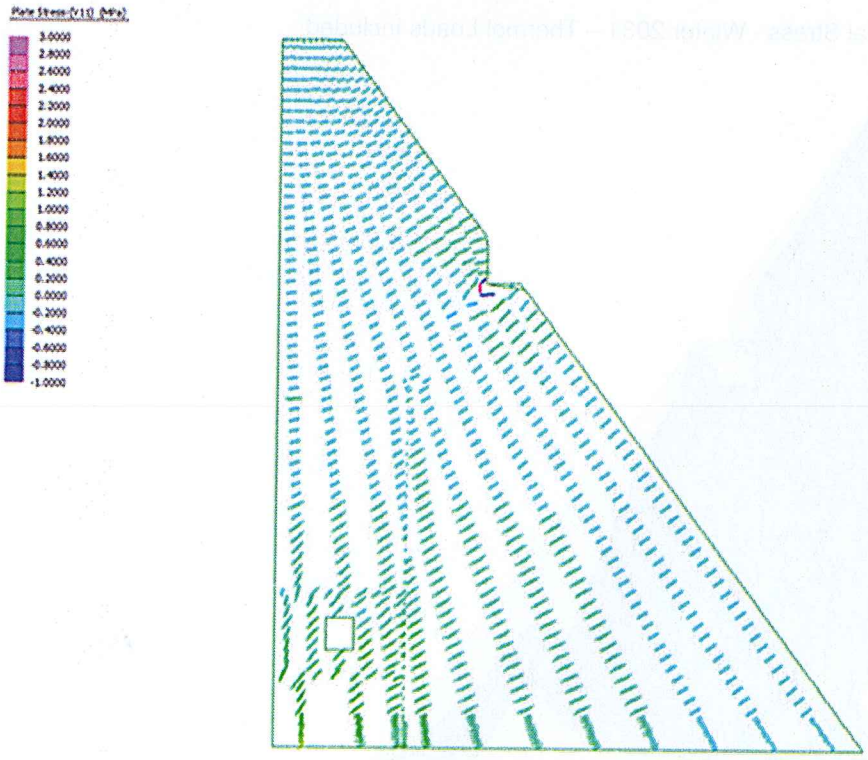

Figure 4.145 Vertical Stress - Winter 2031 – Thermal Loads Excluded

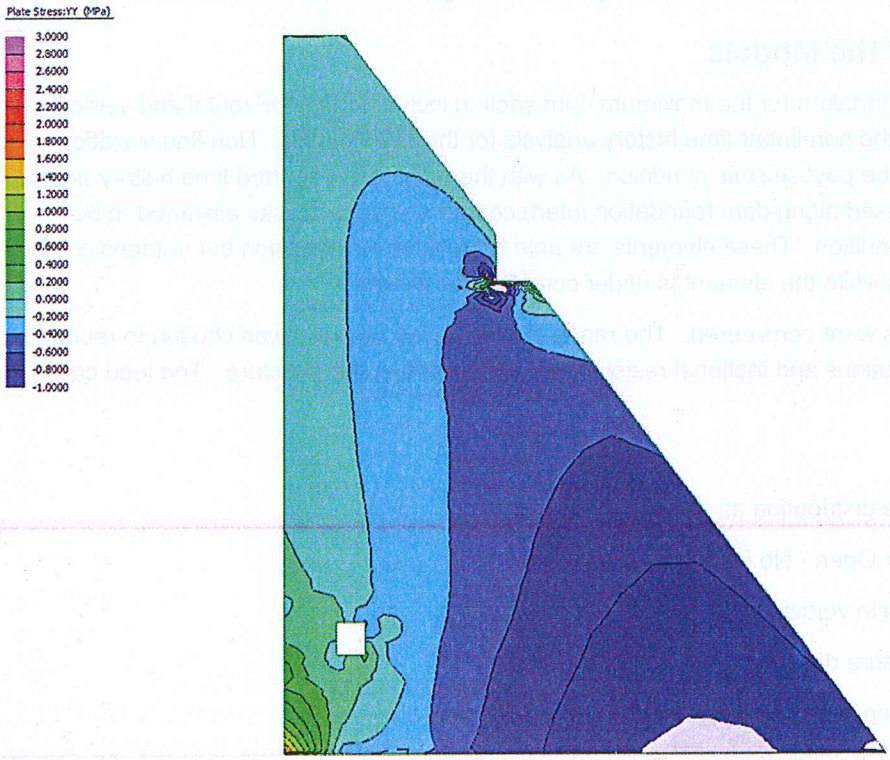

Figure 4.146 Deflected Shape - Winter 2031 -Thermal Load Included

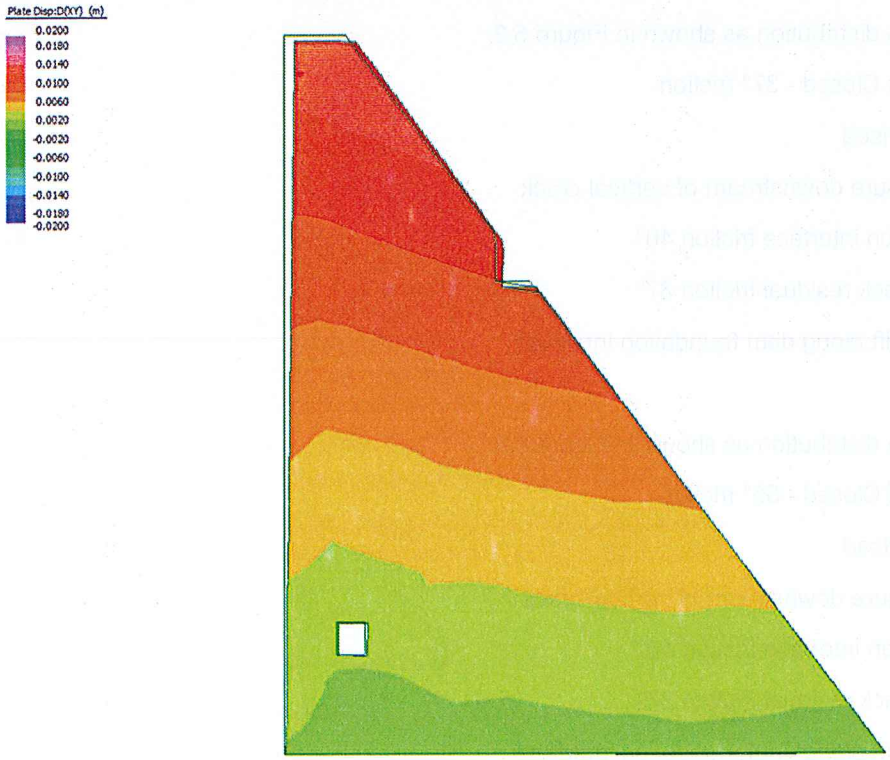

5 Post Seismic Stability Analysis

5.1 Description of the Models

Post seismic analysis was undertaken for the maximum dam section including the horizontal and vertical cracks that were modelled in the non-linear time history analysis for the MDE events. Non-linear static analysis was used to assess the post seismic condition. As with the previously reported time history analysis point contact elements were used along dam foundation interface and along the cracks assumed to be present in the post seismic condition. These elements are able to transfer compression but not tension and can provide friction resistance while the element is under compressive stress.

Three post seismic load cases were considered. The range of load cases selected was chosen to represent possible pore pressure distributions and frictional resistances present within the structure. The load cases can be defined as follows:

- Case 1
  - Pore pressure distribution as shown in Figure 5.1
  - Vertical Crack Open - No friction
  - Free drainage in vertical crack - crack not pressurised
  - No pore pressure downstream of vertical crack
  - Dam foundation interface friction 40°
  - Horizontal Crack residual friction 37°
  - Triangular uplift along dam foundation interface
- Case 2
  - Pore pressure distribution as shown in Figure 5.2
  - Vertical Crack Closed - 37° friction
  - Crack pressurised
  - No pore pressure downstream of vertical crack
  - Dam foundation interface friction 40°
  - Horizontal Crack residual friction 37°
  - Triangular uplift along dam foundation interface
- Case 3
  - Pore pressure distribution as shown in Figure 5.2
  - Vertical Crack Closed - 55° friction
  - Crack pressurised
  - No pore pressure downstream of vertical crack
  - Dam foundation interface friction 40°
  - Horizontal Crack residual friction 37°
  - Triangular uplift along dam foundation interface

5.2 Assumed Pore Pressure Distributions

Two pore pressure distributions have been adopted to assess the post seismic stability. These have been based on the possible crack openings and the assumption of if they are sufficiently open to act as a drain.

5.2.1 Pore Pressure Case 1

In Case 1 it has been assumed that the vertical crack has opened sufficiently that it acts as a drain, and as such no pore pressure is present within the crack. Above and along the horizontal crack the pore pressure is assumed to vary linearly from the reservoir head at the upstream face to atmospheric pressure at the downstream face. Similarly along the dam / foundation interface the pore pressure is assumed to vary linearly from reservoir head at the heal to atmospheric pressure at the toe.

These assumptions introduce some inconsistencies within the pore pressure distribution, in that the drainage capacity of the vertical crack is not considered when developing the pore pressure distribution above the horizontal crack and along the dam / foundation interface. These inconsistencies are not considered to be critical in determining the post seismic stability.

Figure 5.1 Assumed pore pressure distribution for Post Seismic Case 1

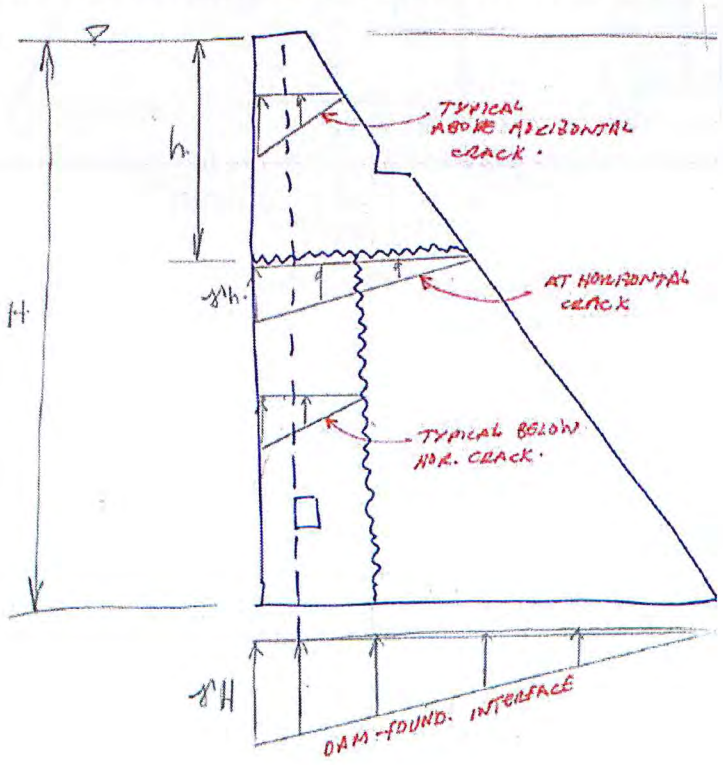

5.2.2 Pore Pressure Case 2

For Case 2 it is assumed that the crack does not open and is therefore capable of retaining pore pressure. Above the horizontal crack and along the dam / foundation interface the pore pressure distribution is identical to that assumed in Case 1. Below the horizontal crack the pore pressure is assumed to vary linearly from the reservoir head at the upstream face to atmospheric pressure on the downstream face.

Along the vertical crack the pressure is assumed to vary linearly from the corresponding pressure in the horizontal crack at the top end of the crack to the corresponding pressure at the dam foundation interface.

Figure 5.2 Assumed pore pressure distribution for Post Seismic Cases 2 and 3

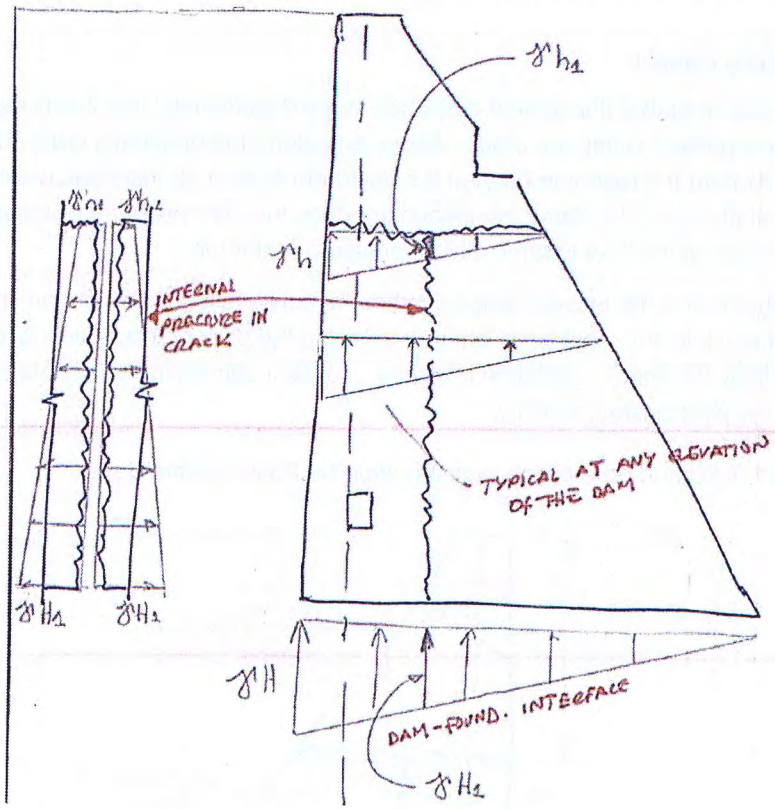

5.3 Modelling Results

Figure 5.3 to Figure 5.11 shows the vertical stress, maximum principal stress and exaggerated displacement plots of the three post seismic load cases considered.

Figure 5.3 Post Seismic Case 1 – Vertical Stress (MPa)

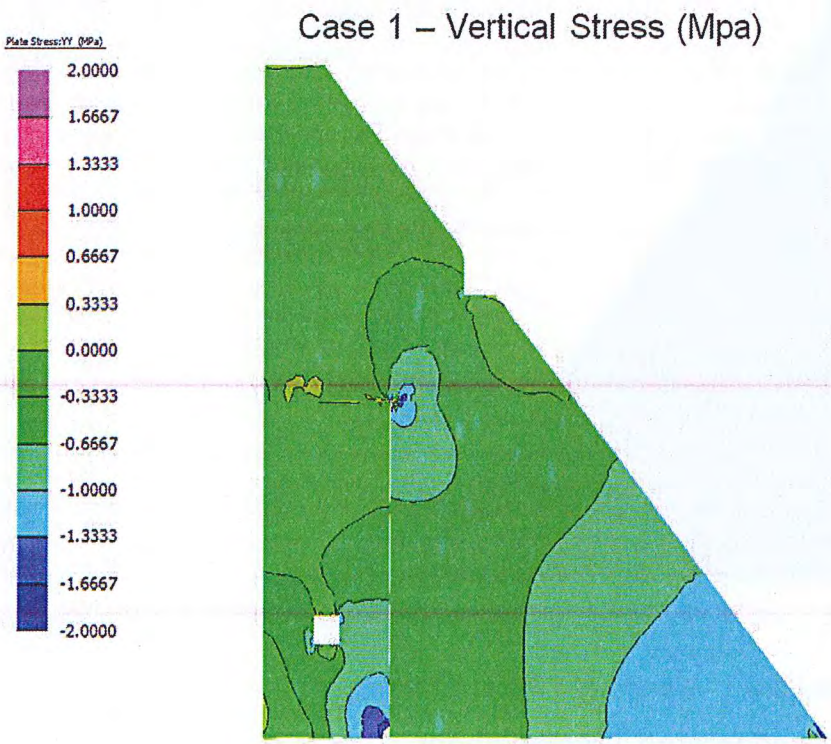

Figure 5.4 Post Seismic Case 1 – Maximum Principal (MPa)

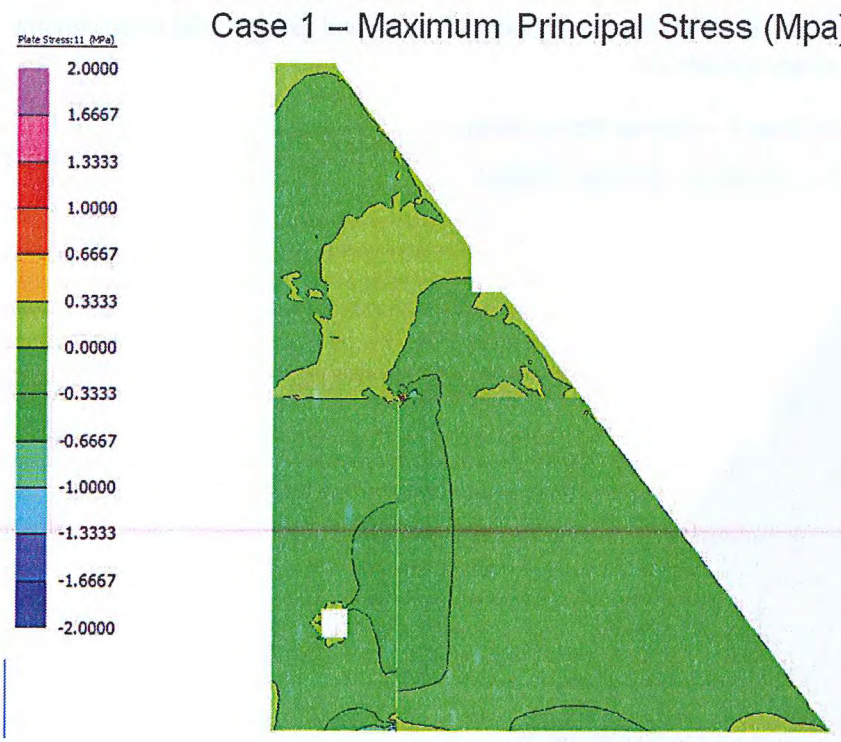

Figure 5.5 Post Seismic Case 1 – Exaggerated Displacement

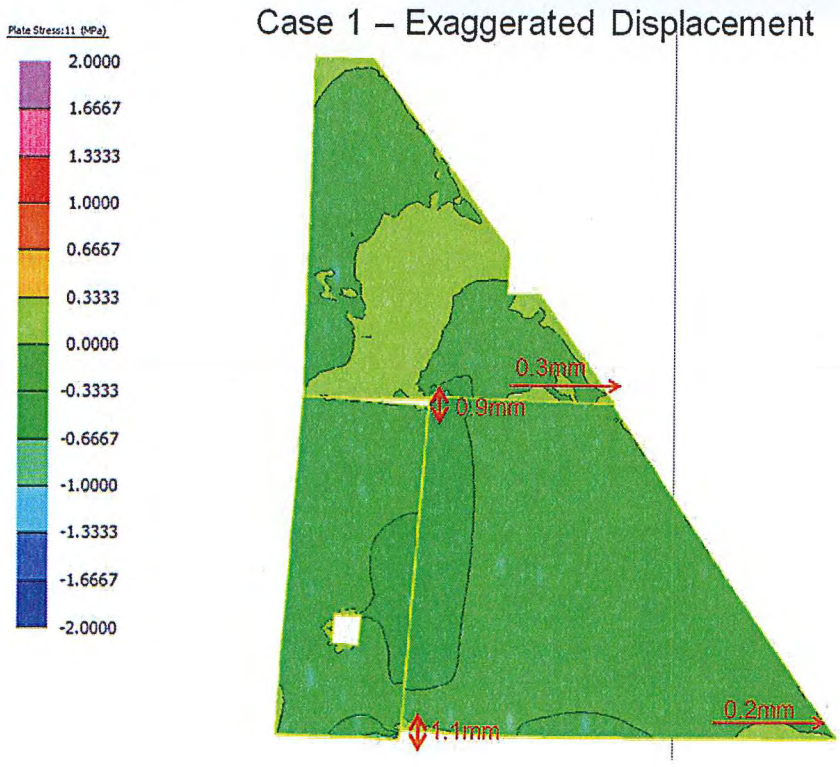

Figure 5.6 Post Seismic Case 2 – Vertical Stress (MPa)

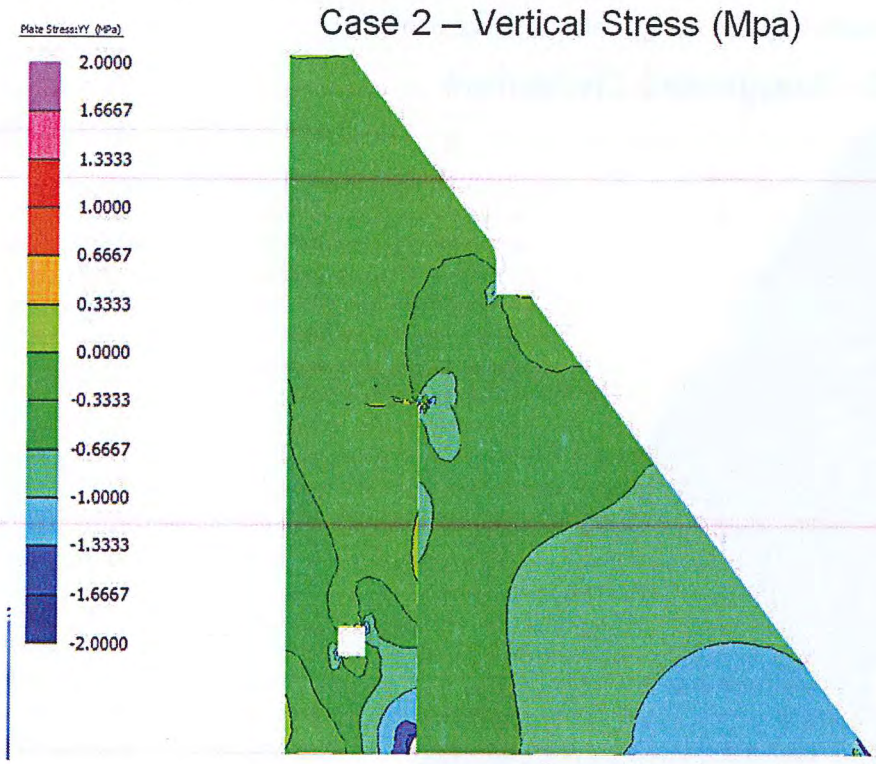

Figure 5.7 Post Seismic Case 2 – Maximum Principal Stress (MPa)

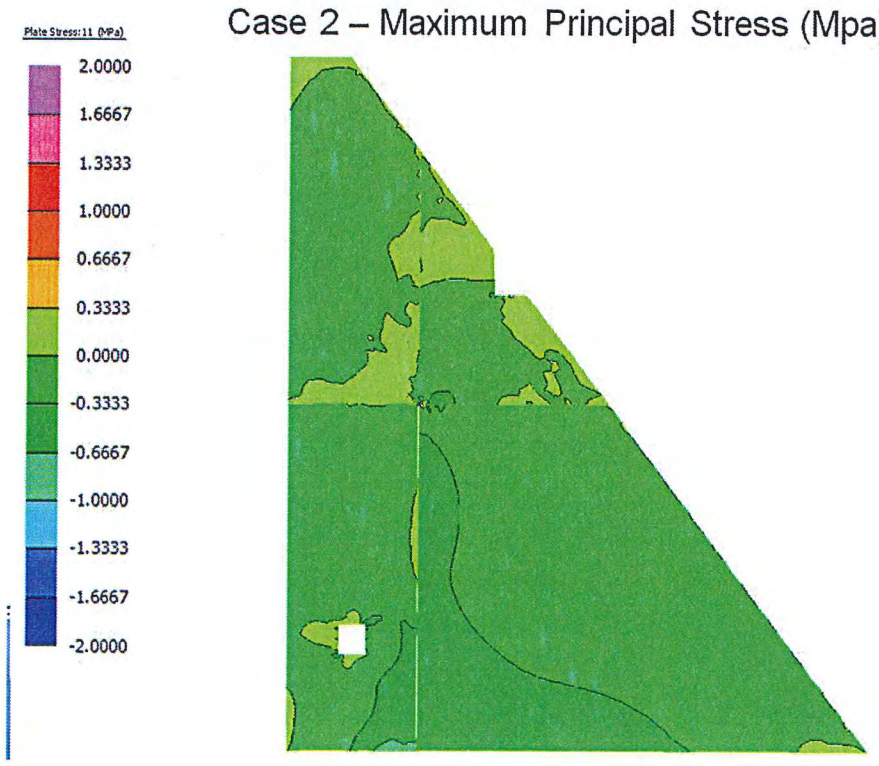

Figure 5.8 Post Seismic Case 2 – Exaggerated Displacement

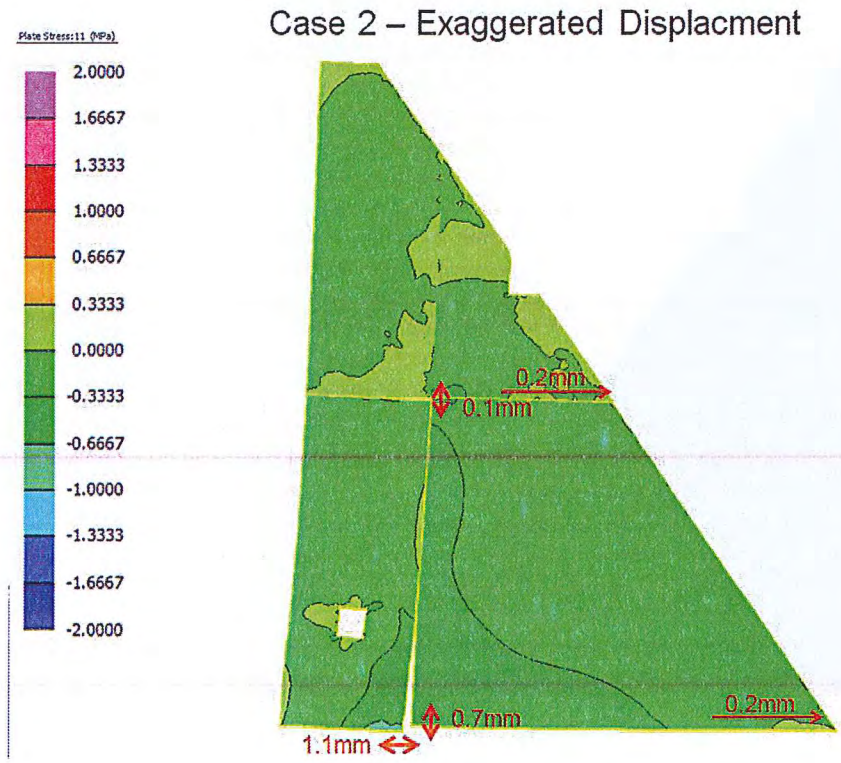

Figure 5.9 Post Seismic Case 3 – Vertical Stress (MPa)

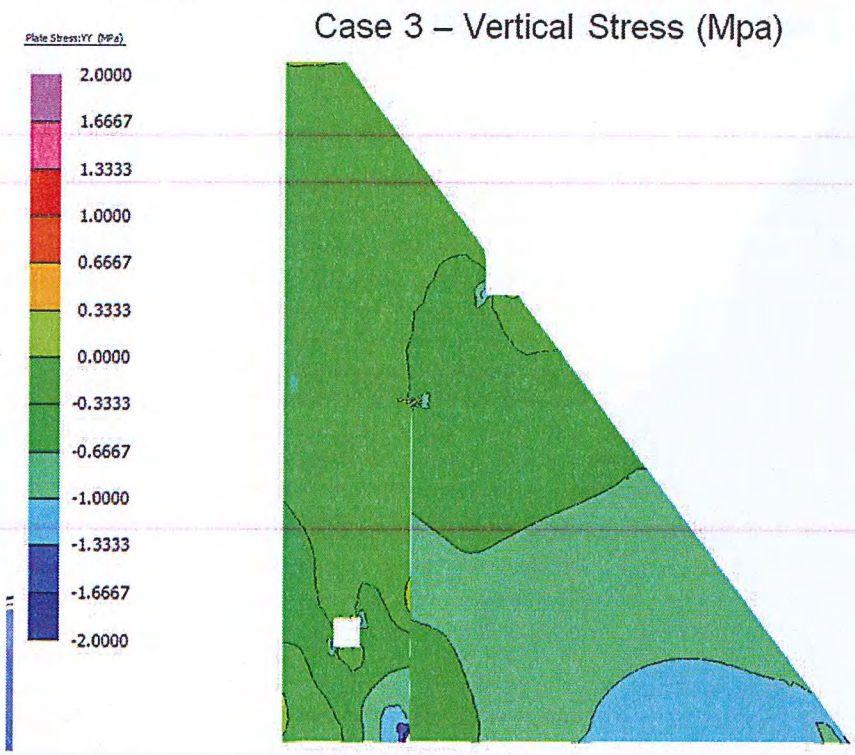

Figure 5.10 Post Seismic Case 3 – Maximum Principal Stress (MPa)

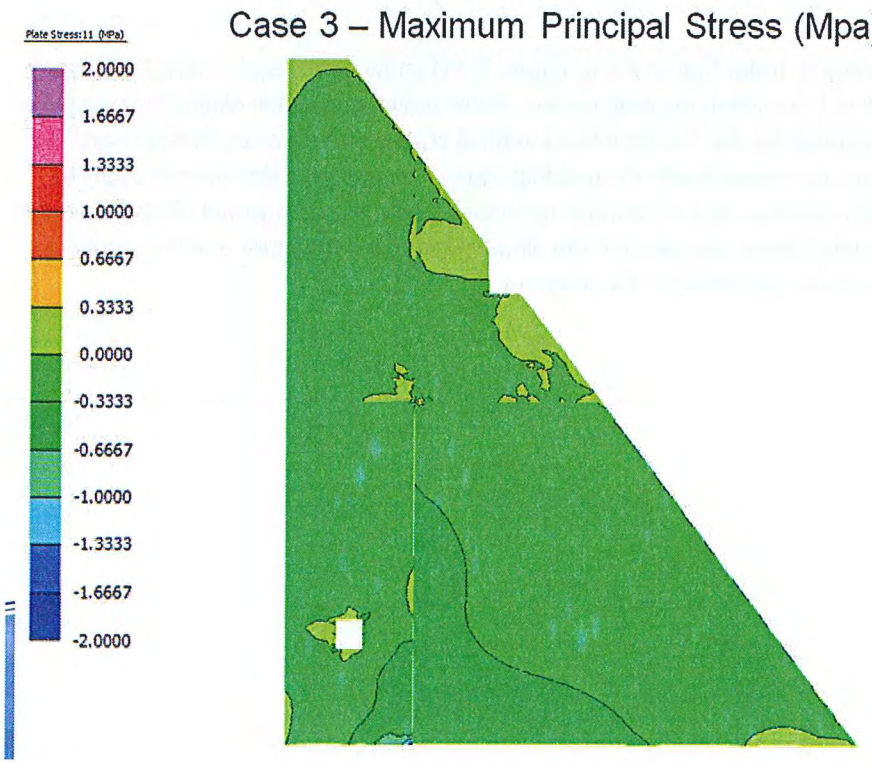

Figure 5.11 Post Seismic Case 3 – Exaggerated Displacement

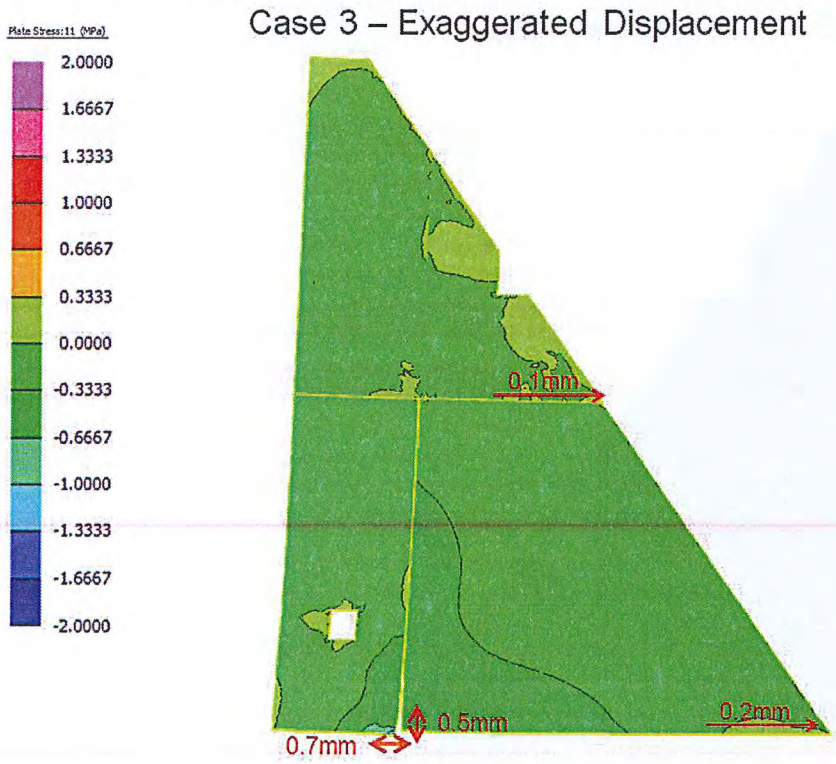

5.4 Discussion

The results of the post seismic analysis (refer Figure 5.3 to Figure 5.11) show no excessive tensile stresses present within the structure for all of the considered load cases. Additionally, only small displacements were observed between the blocks separated by the horizontal and vertical cracks and between the dam and the foundation. If these displacements were added with the residual displacements from the seismic analysis (less than 58 mm at the foundation and less than 42 mm for the upper block) the dam would still be expected to be stable given the size of displacements compared to the dimensions of the structure and the length of the contact between blocks themselves and the dam foundation.

6 Rigid Body Post Seismic Analysis

6.1 Description of the Models

To confirm the results of the FE analysis of the post seismic stability a two dimensional rigid body analysis was undertaken. The dam section adopted is as shown in Figure 5.1 . The analysis assumed that the dam behaves as three individual monoliths, the top part of the dam above RL 511.3 m AHD and the upstream and downstream blocks below RL 511.3 m AHD. Load transfer was assumed along the horizontal crack, however for this analysis it was assumed that no load was transferred across the vertical crack.

The following were assumed for the analysis:-

- Pore pressure distribution as shown in Figure 5.2
- Vertical Crack Open - No friction
- Crack pressurised
- No pore pressure downstream of vertical crack
- Dam foundation interface friction 40°
- Horizontal Crack residual friction 37°
- Triangular uplift along dam foundation interface

The second and third assumptions above are contradictory to those made for the post seismic analysis undertaken in the previous section. However these have been adopted for this analysis as they are considered to be a "worst case".

The stability was assessed for the both the most upstream and downstream locations of the vertical crack.

6.2 Discussion

Upper Section of Dam

The analysis assumed that there is sufficient movement along the horizontal crack surface for the friction angle to reduce to residual, assumed to be 37°. The stability analysis indicated that the upper section had a:-

- Sliding factor of safety of 1.4 and;
- The full length of the base of the section along the cracked surface remained in compression varying from about 300 kPa upstream to about 470 kPa downstream.

Lower Downstream Section

The stability of the lower downstream section was considered for both the most upstream and downstream positions of the vertical crack.

The load transfer from the upper block was assumed to be in proportion with the length of the top section of the lower block, allowing for a linear distribution of the reaction of the upper block. This was applied to both the horizontal and vertical component of the reaction. The stability analysis indicated that the lower downstream section had a:-

Most Upstream Crack:-

- Sliding factor of safety of 1.1 and;

- The full length of the base of the section along the cracked surface remained in compression varying from about 30kPa upstream to about 1,100kPa downstream.

Most Downstream Crack:-

- Sliding factor of safety of 1.2 and;
- The full length of the base of the section along the cracked surface remained in compression varying from about 30kPa upstream to about 1,000kPa downstream.

Therefore the fully cracked dam will remain stable in the post seismic condition, even given the unlikely situation of the vertical crack opening sufficiently that there is no interaction between the upstream and downstream blocks and full hydrostatic head is present within the crack.

7 Conclusion

The main conclusion that can be drawn from the additional time history analysis is as follows:

- Crack Propagation

Subject to the thermal stresses it is unlikely that sufficient tension will be developed to allow the crack to propagate upwards from the RL 511.3 m AHD

It was further shown that the crack is unlikely to propagate downwards more than a few metres below the RL 511.3 m AHD level. However as previous analyses have shown the probable development of reasonably high tensile stresses (<2MPa) as the dam cools it has been conservatively assumed that the dam will crack from RL511.3 m AHD to the foundation for the seismic analysis.

- Linear Analysis

For the OBE events the linear analysis with the inclusion of the crack 15 m from the upstream face demonstrated that the Cotter Dam was both stable and structurally sound. Any possible cracking would likely be relatively minor in nature and be localised to the upstream face at approximately mid height of the dam.

For the MDE events, the stresses were too great in magnitude and area to be adequately assessed through linear analysis. If propagation of the assumed crack were to occur it would possibly connect with cracking along the lift joints between the upstream and downstream faces. As such further non-linear analysis was undertaken to include a possible vertical crack for the MDE events.

- Non-linear Analysis

Results of the nonlinear time-history analysis for the MDE events indicate potential for full crack development at the base and potential cracking along the lift joints. The inclusion of a horizontal crack between the upstream and downstream faces of the dam intercepting the assumed vertical crack at RL 510.8 produces modest residual downstream displacements of the dam. As with the previous uncracked analysis of Cotter Dam the dam is deemed safe to withstand the MDE events but large repairing works would be necessary to reinstate its structural integrity and operational capacity after the earthquake. The inclusion of the assumed vertical crack within the dam does not appear to negatively impact on the dam structural integrity with respect to earthquake loading.

- Post Seismic Analysis

Post seismic analysis undertaken showed that the dam structure would still be stable in post seismic conditions even with the addition of the intersecting horizontal and vertical crack through the maximum height section of the dam.

8 References

1. GHD-ECD-DAM-GN-RPT-1200-0-0, Thermal Analysis, February 2011
2. GHD-ECD-DAM-GN-RPT-1300-0-0, Time History Seismic Analysis, February 2011
3. GHD-ECD-DAM-GN-TMM-003-0-0, ECD Thermal Analysis – 2D Abutment Blocks, February 2012
4. GHD-ECD-DAM-GN-TMM-004-0-0, Thermal Analysis, Cracked Section, May 2012
5. GHD-ECD-DAM-GN-RPT-6103-0-0, Cross Valley Cracking, July 2012